

# The Decomposition of Chemically Activated *n*-Butane, Isopentane, Neohexane, and *n*-Pentane and the Correlation of Their Decomposition Rates with Radical Recombination Rates\*†

W. L. HASE, R. L. JOHNSON,‡ AND J. W. SIMONS

*Chemistry Department, New Mexico State University, Las Cruces, New Mexico 88001*

## Abstract

The total decomposition rates of the chemically activated alkanes *n*-butane, *n*-pentane, isopentane, and neohexane were measured using an internal comparison technique. Chemical activation was by the C—H insertion reaction of excited singlet-state methylene radicals. A total of ten rate constants ranging from  $4.6 \times 10^5$  to  $2.3 \times 10^7$  sec<sup>-1</sup> were measured for these alkanes at different excitation energies. These rates correlate via RRKM theory calculations with thermal *A*-factors in the range of  $10^{16.1}$  to  $10^{17.1}$  sec<sup>-1</sup> for free rotor-activated complex models and in the range of  $10^{16.4}$  to  $10^{17.8}$  sec<sup>-1</sup> for vibrator-activated complex models. It was found that high critical energies for decomposition, "tight" radical models, and activated complex models with free internal rotations were required to correlate the decomposition rates of these alkanes with estimated alkyl radical recombination rates. The correlation is just barely possible even for these favorable extremes, indicating that there may be a basic discrepancy between the recombination rate and decomposition rate data for alkanes.

## 1. Introduction

There have been very few quantitative measurements of the decomposition rates of vibrationally excited alkanes made in other than thermal systems. The decomposition of vibrationally excited ethane, formed by the insertion of singlet methylenes into the C—H bonds of methane, has been studied by Bell and Kistiakowsky [1] and more recently by Halberstadt and McNesby [2]. Whitten and Rabinovitch [3] measured the decomposition rates of chemically activated isobutane and *n*-butane formed by the reaction of methylene with propane. Attempts have been made to correlate the decomposition rates of these alkanes with their respective Arrhenius parameters [3,4], but these attempts have been

---

\* The National Science Foundation is gratefully acknowledged for financial support.

† Abstracted in part from the Ph.D. Thesis of W. L. Hase, New Mexico State University, 1970.

‡ Present address: Chemistry Department, Villanova University, Villanova, Pennsylvania 19085.

generally unsuccessful due to a lack of quantitative information about the level of excitation of the chemically activated species.

Recently, a study of the unimolecular decomposition of chemically activated isobutane and neopentane, formed from the 4358- and 3660-Å photolyses of diazomethane with propane and isobutane, has been reported [5]. RRKM theory calculations were combined with absolute rate theory calculations to determine the Arrhenius parameters for the decomposition paths. It was found that the best correlation of the decomposition rates of the chemically activated isobutane and neopentane with estimated alkyl radical recombination rates requires high critical energies for decomposition, "tight" radical models, and activated complex models with free internal rotations [6]. The average energies of the chemically activated neopentane and isobutane were evaluated using values determined in this laboratory [6,7,8] for the amount of excess energy carried by the singlet methylene into the chemically activated insertion product. The same procedure can be used for the systems in this work.

The purpose of the present research was to obtain accurate experimental decomposition rates for chemically activated *n*-butane, isopentane, *n*-pentane, and neohexane, produced by the C—H insertion reaction of singlet methylene radicals formed from diazomethane photolyses at 4358 and 3660 Å. The total decomposition rates of chemically activated *n*-butane, isopentane, *n*-pentane, and neohexane can be measured utilizing an internal standard to monitor total reaction. The activated complex structures from the earlier study of isobutane and neopentane decomposition should be useful in sorting out the relative contributions of the various possible decomposition paths in the present systems.

## 2. Experimental

### A. Materials

Diazomethane, the methylene radical precursor, was prepared by the reaction of KOH dissolved in 1,4-butanediol with *N*-methyl-*N*-nitroso-*p*-toluenesulfonamide and was stored in di-*n*-butyl phthalate at 77°K. Matheson lecture-bottle propane, *n*-butane, isobutane, and neopentane were purified by gas chromatography, and analyses showed them to be free of impurities. NMR Specialties tetramethylsilane, 99.9% pure, was used without further purification. Trimethylsilane was prepared in vacuo by the reaction of trimethylchlorosilane with LiAlH<sub>4</sub> in dibutyl ether and was purified by gas chromatography. Linde commercial-grade cylinder oxygen was used, and the amount of nitrogen impurity was reduced by distillation at 77°K.

### B. Apparatus and procedure

The apparatus employed was the same as previously described [5]. The range of wavelengths passed by the filters was checked with a Bausch & Lomb Model 33-86-25 monochromator; the energy interval at 4358 Å was 1.5 kcal/mole, and at 3660 Å, it was 0.9 kcal/mole.

Propane-tetramethylsilane-diazomethane, *n*-butane-tetramethylsilane-diazomethane, isobutane-tetramethylsilane-diazomethane, neopentane-trimethylsilane-diazomethane, and neopentane-butane-diazomethane mixtures with added oxygen were photolyzed for times varying from 2 hr at high pressures and up to 30 hr at the lower pressures. All reactions were carried out to less than 5% conversion of the silane and alkane substrates. The ratio of diazomethane to reactants was usually approx. 1.5:10, but no variation in product proportions resulted when this ratio was varied from 1:10 to 3:10. No surface effects were observed by varying reactor volumes for experiments at the same pressure. All the reactions were performed at room temperature. Dark reactions at various pressures gave no interfering products.

### C. Analysis

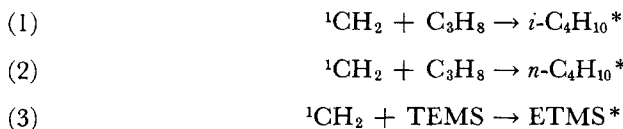
The quantitative analyses of the products condensable at  $-196^{\circ}\text{C}$  were done by gas-liquid phase chromatography. The analytical column consisted of 25 ft of 30% dibutyl phthalate on Chromosorb followed by 4 ft of didecyl phthalate on Chromosorb. The products were identified by mass spectra and GLPC retention times compared with those of known samples. Since the absolute sensitivity factors cancelled out in the determination of the rate constants by the internal standard procedure used in this study, the amounts of the various products were tabulated in terms of the product of their retention times and peak heights.

## 3. Results

### A. Unimolecular decomposition of *n*-butane\* from $^1\text{CH}_2 + \text{C}_3\text{H}_8$ reaction

The reactions of  $^1\text{CH}_2$  with propane and tetramethylsilane (TEMS) mixtures were studied from 0.2 to 130 torr total pressure. The mixtures were photolyzed at 3660 and 4358 Å. In the presence of oxygen, the only significant reaction products with retention times greater than propane were isobutane, *n*-butane, and ethyltrimethylsilane (ETMS). The oxygen-scavenged triplet methylene products and doublet radical products [5] did not come off the column and were not measured. No measurable butane products were formed from either the photolysis of  $\text{CH}_2\text{N}_2$  and  $\text{O}_2$  mixtures or TEMS,  $\text{CH}_2\text{N}_2$ , and  $\text{O}_2$  mixtures.

The insertion reactions which apply to the reaction system under these experimental conditions are given by eqs. (1) to (3):



An asterisk denotes vibrational excitation in the ground electronic state. The ETMS\* formed by reaction (3) is formed at  $\sim 125$  kcal/mole above its ground vibrational state [9]. At the lowest pressure used in these experiments, 0.2 torr, decomposition of ETMS\* amounts to less than 1% [9], and it was used as a con-

venient internal standard for monitoring the total amount of reaction in a given experiment.

The decomposition and stabilization reactions of  $n\text{-C}_4\text{H}_{10}^*$  are given below where the  $\omega$ 's are collisional stabilization rate constants, assuming unit collisional deactivation efficiency:



The decomposition of  $i\text{-C}_4\text{H}_{10}^*$  has been reported [5]. The importance of H-atom rupture and molecular elimination from  $n\text{-C}_4\text{H}_{10}^*$  has been shown to be negligible [3,10,11]. It has been found, for the gas phase radiolysis and photolysis of neopentane, that all alkyl radicals were scavenged by addition of 5% oxygen to the reaction mixture [12]. But, in order to insure that all of the alkyl radicals formed by the decomposition of  $i\text{-C}_4\text{H}_{10}^*$  and  $n\text{-C}_4\text{H}_{10}^*$  were scavenged completely, ~20% oxygen was added to these reaction mixtures. At 0.5 torr, where for the 4358-Å photolyses 74% of the  $i\text{-C}_4\text{H}_{10}^*$  has decomposed, the ETMS/ $i\text{-C}_4\text{H}_{10}$  ratio was unaffected upon increasing the  $\text{O}_2$  in the reaction mixtures to 48%.

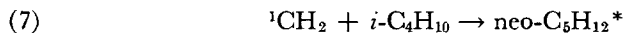
Application of the steady-state approximation to reactions (1) through (6) leads to the following equation, where the product ratio has been normalized to a reactant ratio of 1:

$$(1) \quad \text{ETMS}/n\text{-C}_4\text{H}_{10} = k_3/k_2 + (k_3/k_2) (k_{nB}/\omega)$$

The total rate constant for  $n\text{-C}_4\text{H}_{10}^*$  decomposition is  $k_{nB} = k_4 + k_5$ . A plot of ETMS/ $n\text{-C}_4\text{H}_{10}$  versus  $1/\omega$  should be linear, with the rate constant for decomposition given by the slope divided by the intercept. Plots based on such a treatment are shown in Figure 1 for the two photolyses wavelengths. A summary of the rate constants deduced is given in Table I.

#### B. Unimolecular decomposition of isopentane\* from $^1\text{CH}_2 + i\text{-C}_4\text{H}_{10}$ reaction

The photolysis of diazomethane, at 3660 and 4358 Å, in mixtures of isobutane and TEMS in the presence of oxygen was studied from 0.1 to 200 torr. The major products were neopentane, isopentane, and ETMS. Approximately 15% oxygen was added to these reaction mixtures. The largest amount of decomposition of the chemically activated neopentane and isopentane was 57% and 47%, respectively. At the lowest pressures used in these experiments, less than 2% of the ETMS\* decomposed [9], and thus it was suitable as an internal standard. The following reaction scheme accounts for the formation and ensuing decomposition and stabilization of the chemically activated isopentane:



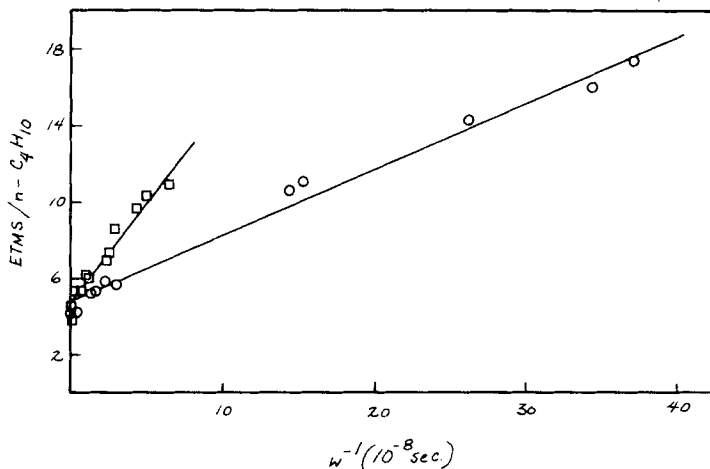
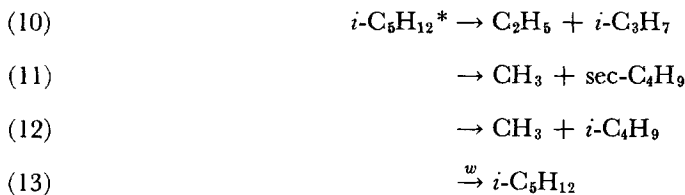


Figure 1. Plot of ETMS/ $n\text{-C}_4\text{H}_{10}$  vs.  $1/w$  for the TEMS/ $\text{C}_3\text{H}_8$ / $\text{CH}_2\text{N}_2$ / $\text{O}_2$  photolyses: (□) photolysis at 3660 Å; (○) photolysis at 4358 Å. The lines were determined by the method of least squares.



The decomposition of neo- $\text{C}_5\text{H}_{12}^*$  has been described [5].

Application of the steady-state approximation to reactions (7) through (13) leads to eq. (2):

$$(2) \quad \text{ETMS}/i\text{-C}_5\text{H}_{12} = k_9/k_8 + (k_9/k_8) (k_{IP}/w)$$

where  $k_{IP} = k_{10} + k_{11} + k_{12}$  and the product ratio has been normalized to a reactant ratio of 1. Plots of the data for  $i\text{-C}_5\text{H}_{12}^*$  decomposition are given in Figure 2. A summary of the deduced rate constants is given in Table I.

### C. Unimolecular decomposition of isopentane\* and n-pentane\* from $^1\text{CH}_2 + n\text{-C}_4\text{H}_{10}$ reaction

Mixtures of diazomethane,  $n$ -butane, and TEMS with added oxygen were photolyzed at 3660 and 4358 Å. For most of the experiments,  $\sim 15\%$  oxygen was added to the reaction mixtures, but for the reactions at the lower pressures,  $\sim 20\%$  oxygen was added to the reaction mixtures. The products formed other than those from diazomethane decomposition were  $i\text{-C}_5\text{H}_{12}$ ,  $n\text{-C}_5\text{H}_{12}$ , and ETMS. The maximum decomposition of  $i\text{-C}_5\text{H}_{12}^*$  and  $n\text{-C}_5\text{H}_{12}^*$  was 56% and 46%, respec-

TABLE I. Summary of experimental rate constants.

| Molecule          | Formation reaction                            | Wavelength of $\text{CH}_2\text{N}_2$ Interphotolysis, Å |      | Experimental Decomposition Rate Constants <sup>a</sup> |                             |
|-------------------|---|--|------|--|-----------------------------|
|                   |   |  |      | $k$ , torr   | $k$ , $\text{sec}^{-1}$     |
| <i>n</i> -Butane  | $^1\text{CH}_2 + \text{C}_3\text{H}_8$        | 3660   | 4.60 | 1.06   | $(2.3 \pm 0.2) \times 10^7$ |
| <i>n</i> -Butane  |   | 4358   | 4.75 | 0.35 <sup>b</sup>                                      | $(7.3 \pm 0.6) \times 10^6$ |
| Isopentane        | $^1\text{CH}_2 + i\text{-C}_4\text{H}_{10}$   | 3660   | 2.49 | 0.13   | $(3.1 \pm 0.2) \times 10^6$ |
| Isopentane        |   | 4358   | 2.54 | 0.071  | $(1.6 \pm 0.1) \times 10^6$ |
| Isopentane        | $^1\text{CH}_2 + n\text{-C}_4\text{H}_{10}$   | 3660   | 3.86 | 0.12   | $(2.8 \pm 0.1) \times 10^6$ |
| Isopentane        |   | 4358   | 3.81 | 0.091  | $(2.2 \pm 0.1) \times 10^6$ |
| <i>n</i> -Pentane | $^1\text{CH}_2 + n\text{-C}_4\text{H}_{10}$   | 3660   | 3.52 | 0.079  | $(1.8 \pm 0.1) \times 10^6$ |
| <i>n</i> -Pentane |   | 4358   | 3.52 | 0.066  | $(1.5 \pm 0.1) \times 10^6$ |
| Neohexane         | $^1\text{CH}_2 + \text{neo-C}_5\text{H}_{12}$ | 3660   | —    | 0.033  | $(8.7 \pm 1.2) \times 10^5$ |
| Neohexane         |   | 4358   | —    | 0.017  | $(4.6 \pm 0.8) \times 10^5$ |

<sup>a</sup> The rate constants in torr units refer to the average bath pressure where one half of the activated molecules are stabilized. These values were calculated from the rate constants in  $\text{sec}^{-1}$  units for an average set of partial pressures and are tabulated since they are for many purposes more descriptive than the rate constants in  $\text{sec}^{-1}$  units.

<sup>b</sup> This value agrees fairly well with the value reported by Whitten and Rabinovitch [3].

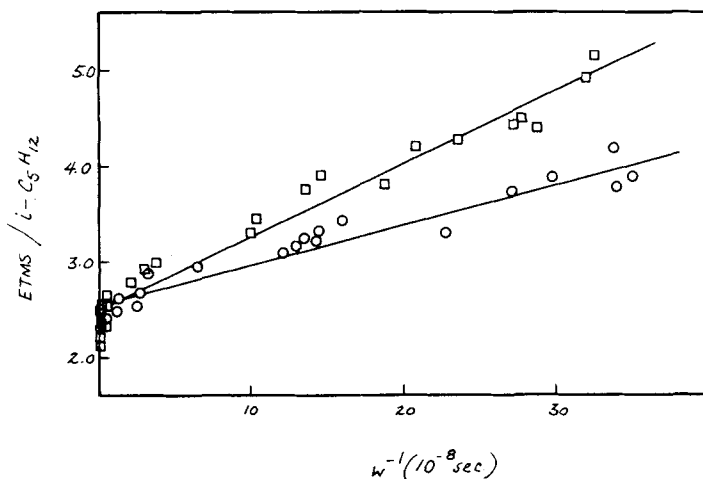
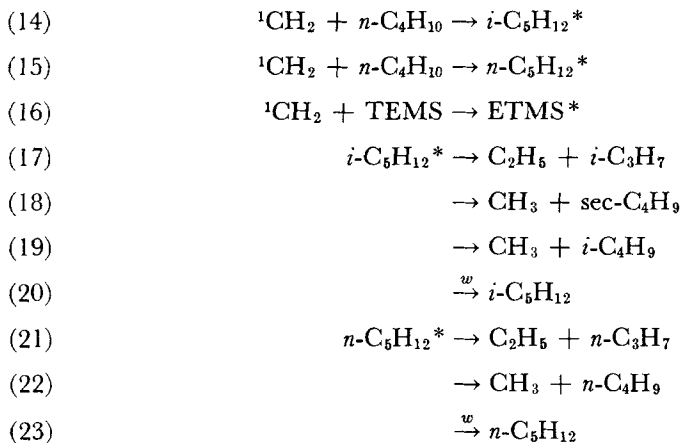


Figure 2. Plot of  $\text{ETMS}/i\text{-C}_5\text{H}_{12}$  vs.  $1/w$  for the  $\text{TEMS}/i\text{-C}_4\text{H}_{10}/\text{CH}_2\text{N}_2/\text{O}_2$  photolyses: (□) photolysis at 3660 Å; (○) photolysis at 4358 Å. The lines were determined by the method of least squares.

tively. The products formed in this system can be accounted for by the following reaction scheme:



ETMS\* was again suitable as an internal standard. Applying the steady-state approximation to reactions (14) through (23) and normalizing the product ratios to a reactant ratio of 1 leads to the following two equations:

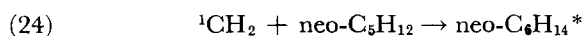
$$(3) \quad \text{ETMS}/i\text{-C}_5\text{H}_{12} = k_{16}/k_{14} + (k_{16}/k_{14}) (k_{IP}/w)$$

$$(4) \quad \text{ETMS}/n\text{-C}_5\text{H}_{12} = k_{16}/k_{15} + (k_{16}/k_{15}) (k_{nP}/w)$$

where  $k_{IP} = k_{17} + k_{18} + k_{19}$ , and  $k_{nP} = k_{21} + k_{22}$ . Plots of ETMS/ $i\text{-C}_5\text{H}_{12}$  versus  $1/w$  are shown for the 4358- and 3660-Å diazomethane photolyses in Figure 3. The plots of ETMS/ $n\text{-C}_5\text{H}_{12}$  versus  $1/w$  are in Figure 4. The rate constants derived from these plots for  $n$ -pentane\* and isopentane\* decomposition are given in Table I.

#### D. Unimolecular decomposition of neohexane\* from ${}^1\text{CH}_2 + (\text{CH}_3)_4\text{C}$ reaction

Ethyltrimethylsilane\* decomposes appreciably in the pressure range where neohexane\* decomposes, thus it could not be used as an internal standard to monitor neohexane\* decomposition. A related technique can be used. A chemically activated molecule which has a rate of decomposition similar to that of neohexane\* can serve as an internal standard if its decomposition rate is known. This idea was used to monitor neohexane\* decomposition, where ethyldimethylsilane\* (EDMS\*), formed by the  ${}^1\text{CH}_2 + \text{trimethylsilane (TMS)}$  reaction, and both isopentane\* and  $n$ -pentane\*, formed by the  ${}^1\text{CH}_2 + n\text{-butane}$  reaction, served as internal standards. The reactions pertinent to the formation and decomposition of neohexane\* with ethyldimethylsilane\* as an internal standard are given below:



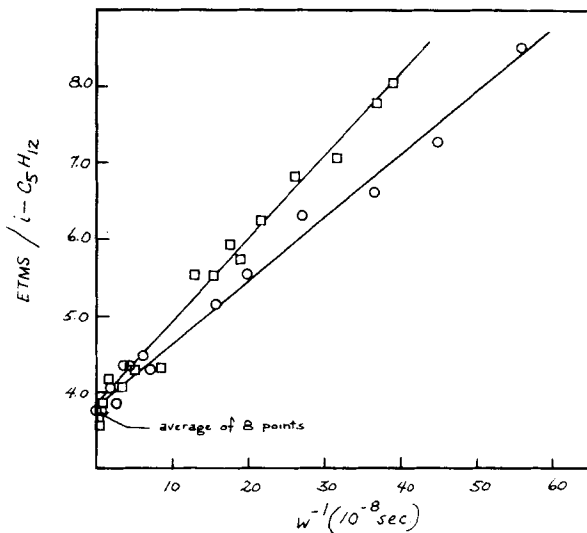
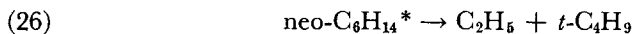


Figure 3. Plot of  $ETMS/i-C_5H_{12}$  vs.  $1/w$  for the  $TMS/n-C_4H_{10}/C_4H_2N_2/O_2$  photolyses: ( $\square$ ) photolysis at  $3660 \text{ \AA}$ ; ( $\circ$ ) photolysis at  $4358 \text{ \AA}$ . The lines were determined by the method of least squares.



Applying the steady-state approximation to the preceding mechanism and normalizing the product ratios to a reactant ratio of 1, one obtains the following equation:

$$(5) \quad (\text{EDMS}/\text{neo-C}_6\text{H}_{14}) (1 + k_{\text{EDMS}}/w) = k_{26}/k_{24} + (k_{25}/k_{24}) (k_{\text{NH}}/w)$$

where  $k_{\text{NH}} = k_{26} + k_{27} + k_{28}$ . With isopentane\* and *n*-pentane\* as internal standards, the reactions and equation are similar, except that *n*-butane replaces TMS. The decomposition rate of EDMS\* is  $2.2 \times 10^5 \text{ sec}^{-1}$  and  $4.3 \times 10^5 \text{ sec}^{-1}$  at 4358 and 3660  $\text{\AA}$ , respectively [9]. Using these values for  $k_{\text{EDMS}}$ , plots of the left-hand side of eq. (5) versus  $1/w$  for the photolyses at 4358 and 3660  $\text{\AA}$  are shown in Figure 5. The rate constant for isopentane\* decomposition is  $2.2 \times 10^6 \text{ sec}^{-1}$  at 4358  $\text{\AA}$  and  $2.8 \times 10^6 \text{ sec}^{-1}$  at 3660  $\text{\AA}$ , and the rate constant for *n*-pentane\* decomposition is  $1.5 \times 10^6 \text{ sec}^{-1}$  at 4358  $\text{\AA}$  and  $1.85 \times 10^6 \text{ sec}^{-1}$  at 3660  $\text{\AA}$ , as determined earlier. Using these decomposition rate constants, plots of  $(i\text{-C}_5\text{H}_{12}/$

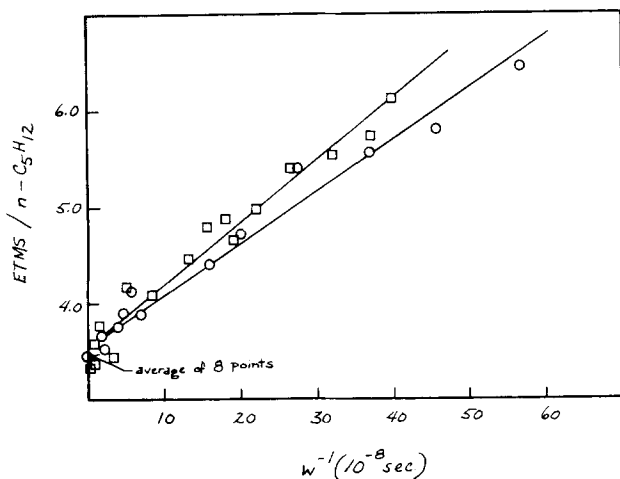


Figure 4. Plot of  $ETMS/n-C_5H_{12}$  vs.  $1/w$  for the  $TMS/n-C_4H_{10}/CH_2N_2/O_2$  photolyses: ( $\square$ ) photolysis at  $3660 \text{ \AA}$ ; ( $\circ$ ) photolysis at  $4358 \text{ \AA}$ . The lines were determined by the method of least squares.

$NH$ )  $(1 + k_{IP}/w)$  versus  $1/w$  are shown in Figure 6, and plots of  $(n-C_5H_{12}/NH)$   $(1 + k_{nP}/w)$  versus  $1/w$  are shown in Figure 7 for the  $4358$ - and  $3660\text{-\AA}$  photolyses. The three experimental values of  $k_{NH}$  thus determined at each wavelength were averaged and are summarized in Table I.

#### E. Discussion of experimental rate constants

The intercepts and slopes of Figures 1 to 7 were evaluated by the method of least squares. The error limits listed for the rate constants in Table I, except those for neohexane\*, represent the combined probable errors (50% confidence limits) in the slopes and intercepts. It is seen for most of the rate constants the error is less than 10%, which indicates a good fit of the "least squares" lines to the data. The error limits given for the average neohexane\* decomposition rate constants were chosen so they would encompass the three experimental determinations of the rate constants. The results given in ref. [6] indicate that there should be no difference in the intercepts of the two lines, for the  $4358$ - and  $3660\text{-\AA}$  photolyses. The maximum deviation from this prediction, as seen from Table I, is for the decomposition of  $n$ -butane where there is a 3% difference in the intercepts.

It is seen from Table I that the rate constants get smaller as the number of degrees of freedom in the molecules are increased. Since all of these molecules are produced at nearly the same level of vibrational excitation, and have nearly the same critical energies for decomposition (a detailed discussion of the energetics of these molecules is given in the next section), this effect must be due to the excess energy being distributed among all the vibrational degrees of freedom and thus a lower probability of the critical energy being found in the reaction path as the degrees of freedom are increased.

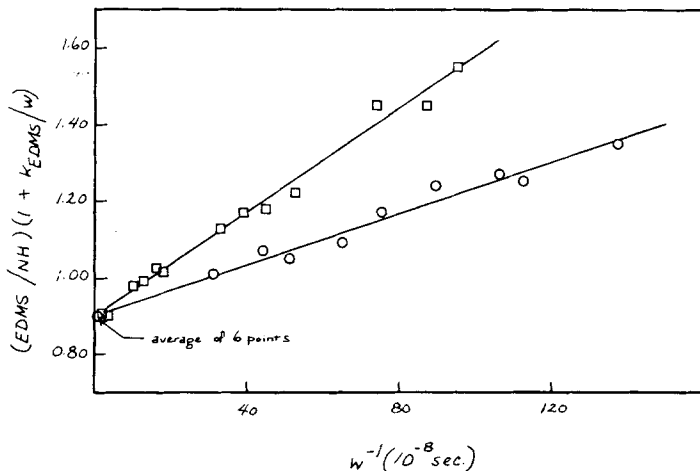


Figure 5. Plot of  $(EDMS/NH)(1 + k_{EDMS}/w)$  vs.  $1/w$  for the TRMS/neo-C<sub>5</sub>H<sub>12</sub>/CH<sub>2</sub>N<sub>2</sub>/O<sub>2</sub> photolyses: (□) photolysis at 3660 Å; (○) photolysis at 4358 Å.  $k_{EDMS}$  equals  $4.3 \times 10^5 \text{ sec}^{-1}$  and  $2.2 \times 10^5 \text{ sec}^{-1}$  for the 3660-Å and 4358-Å photolyses, respectively. The lines were determined by the method of least squares.

The calculation of the collision frequencies required values for the molecular diameters of the various molecules. Since molecular diameters have not been measured for the alkylsilanes, they were approximated here by assuming that a Si atom contributes as much to the collision diameter of a molecule as two carbon atoms in a similar alkane. The effective Lennard-Jones collision diameters for the alkanes were determined from hard-sphere values by the method described by Rabinovitch et al. [13,14]. The effective pressure of oxygen was taken to be 0.25 of the measured pressure due to its lower collisional deactivation efficiency [15]. The collision diameters used are listed in Appendix I. These collision diameters are consistent with the values used by Simons and Taylor [7,8] in the determination of the quantity,  $E^*(^1\text{CH}_2) + \Delta H_{10}^0(^1\text{CH}_2)$ , which will be used in the theoretical calculations section.

#### 4. Theoretical Calculations

##### A. RRKM and absolute rate theory

The Rice-Ramsperger-Kassel-Marcus (RRKM) [4,17-19] theory expression for the decomposition rate  $k_{E^*}$  of a molecule at energy  $E^*$  is given in eq. (6):

$$(6) \quad k_{E^*} = \frac{d}{h} \frac{\sum_{E_{VR}^+} P(E_{VR}^+)}{N(E^*_{VR})}$$

where  $\sum_{E_{VR}^+} P(E_{VR}^+)$  is the sum of all vibrational-internal rotational energy

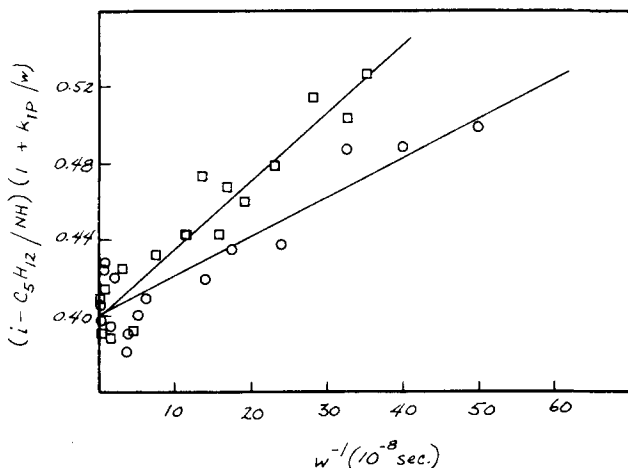


Figure 6. Plot of  $(i\text{-C}_5\text{H}_{12}/\text{NH})(1 + k_{\text{IP}}/w)$  vs.  $1/w$  for the  $n\text{-C}_4\text{H}_{10}/\text{neo-C}_5\text{H}_{12}/\text{CH}_2\text{N}_2/\text{O}_2$  photolyses: (□) photolysis at 3660 Å; (○) photolysis at 4358 Å.  $k_{\text{IP}}$  equals  $2.8 \times 10^6 \text{ sec}^{-1}$  and  $2.2 \times 10^6 \text{ sec}^{-1}$  for the 3660-Å and 4358-Å photolyses, respectively. The lines were determined by the method of least squares.

eigenstates for the activated complex up to the energy  $E^+$ , and  $E^+ = E^* - E_0 + \langle E_J \rangle - \langle E_{J^+} \rangle$ . The critical energy for dissociation is  $E_0$ , and  $\langle E_J \rangle - \langle E_{J^+} \rangle$  is the difference in energy for the adiabatic modes (overall rotations) of the energized molecule and activated complex. For rigid activated complexes,  $\langle E_J \rangle$  and  $\langle E_{J^+} \rangle$  are normally about equal, but for loose activated complexes leading to dissociation,  $\langle E_J \rangle$  and  $\langle E_{J^+} \rangle$  differ primarily for two overall rotations, and the mean value of  $\langle E_J \rangle - \langle E_{J^+} \rangle$  is equal to  $(I^+/I - 1)(RT/2)$ , where  $l$  is the number of adiabatic rotations and  $I^+/I$  is the ratio of the product of the moments of inertia for these rotations.  $N(\langle E_{\text{VR}}^* \rangle)$  is the density of the vibrational-internal rotational energy eigenstates for the activated molecule,  $d$  is the reaction path degeneracy, and  $h$  is Planck's constant. The thermal distribution of energies for the chemically activated molecules of this study is narrow enough so that an essentially monoenergetic species is formed. Thus no integration of  $k_{E^*}$  over the thermal spread  $f(E_{\text{VR}}^*)$  was carried out, but instead  $k_{\langle E^* \rangle}$  at the average energy  $\langle E^* \rangle$  was compared with the experimental values. The initially formed excited molecules have an energy spread of  $\sim 10$  kcal/mole due to photolysis and thermal energy distributions in the formation reactions; but since the average excess energy, given by  $\langle E^+ \rangle = \langle E^* \rangle - E_0 \cong 120 - 80 \cong 40$  kcal/mole, is also large, the relative dispersion is small; e.g.,  $k_{a0}/k_{a0} \cong 1.5$ . Thus the experimental rate constants are well represented by  $k_{\langle E^* \rangle}$  values [20,21]. The sums of the vibrational-internal rotational states for the activated complexes and the densities of the vibrational-internal rotational states for the molecules were calculated using the approximation developed by Whitten and Rabinovitch [22]. The computations were done on either a CDC-3300 or IBM-360 computer. Arrhenius parameters were calculated from standard ART expressions [23].

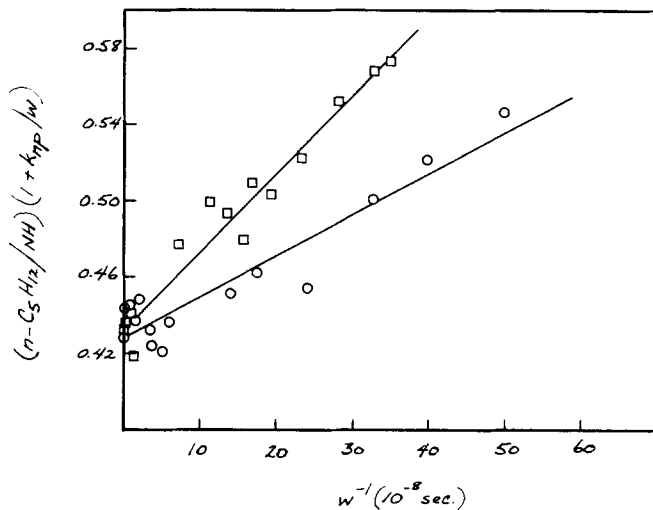


Figure 7. Plot of  $(n\text{-C}_5\text{H}_{12}/\text{NH})(1 + k_{\text{NP}}/w)$  vs.  $1/w$  for the  $n\text{-C}_4\text{H}_{10}/\text{neo-C}_5\text{H}_{12}/\text{CH}_2\text{N}_2/\text{O}_2$  photolyses: ( $\square$ ) photolysis at 3660 Å; ( $\circ$ ) photolysis at 4358 Å.  $k_{\text{NP}}$  equals  $1.85 \times 10^6 \text{ sec}^{-1}$  and  $1.5 \times 10^6 \text{ sec}^{-1}$  for the 3660-Å and 4358-Å photolyses, respectively. The lines were determined by the method of least squares.

### B. Thermochemistry

The excitation energy  $\langle E^* \rangle$  is given by the following equation:

$$(7) \quad \langle E^* \rangle = E^*(^1\text{CH}_2) + \Delta H_{\text{f}_0}^0(^1\text{CH}_2) + \Delta H_{\text{f}_0}^0(\text{A}) - \Delta H_{\text{f}_0}^0(\text{CH}_2\text{A}) + E_{\text{th}}$$

where  $E^*(\text{CH}_2)$  is the excess energy carried by the singlet methylene from the photolysis reaction into the chemically activated product  $\text{CH}_2\text{A}^*$ ,  $E_{\text{th}}$  is the average thermal energy of the reactants  $^1\text{CH}_2$  and A, and the other quantities are the appropriate 0°K enthalpies of formation.

For the alkanes studied here, the heats of formation at 0°K are accurately known, and the values are listed in various tables [24]. The values of  $E_{\text{th}}$  were calculated from statistical thermodynamics. The quantity  $E^*(^1\text{CH}_2) + \Delta H_{\text{f}_0}^0(^1\text{CH}_2)$  has been determined by Simons and Taylor for diazomethane-*cis*-butene-2 photolyses at 3660 and 4358 Å [7,8], where the values are 116.1 and 112.6 kcal/mole, respectively. It is felt that these values are accurate to within  $\pm 2$  kcal/mole [7]. These values are applicable to the alkane systems studied here if the total intrinsic reactivities of the various alkane reactants toward singlet methylene reaction is the same as that for *cis*-butene-2. The results of ref. [6] indicate that the total intrinsic reactivity of *cis*-butene-2 is virtually the same as those for propane, *n*-butane, isobutane, and neopentane. These values of  $E^*(^1\text{CH}_2) + \Delta H_{\text{f}_0}^0(^1\text{CH}_2)$  were determined by Simons and Taylor by equating  $k_{\langle E^* \rangle}$  with  $k_a$  for the geometric and structural isomerization rates of chemically activated *cis*-1,2-dimethylcyclopropane. The use of these values would in effect

cancel any errors resulting from equating  $k_{<B^*>}$  with  $k_a$  in the calculations presented here.

The other energy quantities which are essential to the evaluation of  $k_{<B^*>}$  are the critical energies for the different C—C bond ruptures which can be obtained from the appropriate C—C bond dissociation energies corrected to 0°K. Bond dissociation energies for various types of C—C bonds have been measured to within about 2 kcal/mole, and they are given in Table II [25–28].

TABLE II. C—C Bond dissociation energies.

| Reaction path     |   | $D_{298}^0, \pm 2$ kcal/mole |
|-------------------|---|------------------------------|
| Isobutane         | $\longrightarrow \text{CH}_3 + i\text{-C}_3\text{H}_7$          | 83                           |
| <i>n</i> -Butane  | $\longrightarrow 2\text{C}_2\text{H}_5$                         | 82                           |
| <i>n</i> -Butane  | $\longrightarrow \text{CH}_3 + n\text{-C}_3\text{H}_7$          | 85                           |
| Neopentane        | $\longrightarrow \text{CH}_3 + t\text{-C}_4\text{H}_9$          | 80                           |
| Isopentane        | $\longrightarrow \text{C}_2\text{H}_5 + i\text{-C}_3\text{H}_7$ | 80                           |
| Isopentane        | $\longrightarrow \text{CH}_3 + \text{sec-C}_4\text{H}_9$        | 83                           |
| Isopentane        | $\longrightarrow \text{CH}_3 + i\text{-C}_4\text{H}_9$          | 85                           |
| <i>n</i> -Pentane | $\longrightarrow \text{C}_2\text{H}_5 + n\text{-C}_3\text{H}_7$ | 82                           |
| <i>n</i> -Pentane | $\longrightarrow \text{CH}_3 + n\text{-C}_4\text{H}_9$          | 85                           |
| Neohexane         | $\longrightarrow \text{C}_2\text{H}_5 + t\text{-C}_4\text{H}_9$ | 77                           |
| Neohexane         | $\longrightarrow \text{CH}_3 + t\text{-C}_5\text{H}_{11}$       | 80                           |
| Neohexane         | $\longrightarrow \text{CH}_3 + \text{neo-C}_5\text{H}_{11}$     | 85                           |

### C. Activated complex structures

Models for activated complexes which have been used in the calculation of thermal Arrhenius *A*-factors for C—C bond rupture in alkanes have been constructed previously from the molecule by lowering four of the following motions: methyl rocking, methylene rocking, and skeletal bending [3,4,29–31]. The activated complex for ethane decomposition has been constructed by lowering the four rocking modes of the two methyl groups [4,29,31], and the activated complex structure for ethyl rupture from *n*-butane has been constructed by lowering two CH<sub>2</sub> rocking motions and two C—C—C bending motions [3]. A similar general approach has been taken in this work. Four rocking and bending vibrations in the activated complexes were adjusted in order to make the theoretical rates fit the experimental decomposition rates. A C—C stretching vibration was taken as the reaction coordinate in all cases. The torsion modes were treated as both low-frequency vibrators and as free rotors to determine which treatment gives the best correlation between the decomposition and estimated recombination rates.

$I^+/I$  was taken to be 4 for all the reaction paths which corresponds to lengthening the C—C bond by a factor of  $\sim 2$  in the activated complex. Such a lengthening has been used previously in similar calculations for ethane [4,32] and *n*-butane [4] decomposition. The fundamental molecular frequencies for the molecules were taken from Snyder and Schachtschneider [33,34].

#### D. Radical structures

The methyl radical is the only alkyl radical for which the vibrational frequencies have been measured and structure has been determined [35]. The vibrational frequencies for the rest of the alkyl radicals have been assigned here by comparison to related hydrocarbon molecules. It was assumed that the carbon atom bearing the unpaired electron was  $sp^2$  hybridized while the remaining carbons were  $sp^3$  hybridized.

The barriers to internal rotation in the alkanes are significant, 3.0 kcal/mole in ethane [36] and 4.3 kcal/mole in neopentane [37,38], but ESR [39] and NMR [40] investigations of alkyl radicals indicate that barriers to internal rotation about bonds adjacent to the unpaired electron in alkyl radicals are very small. The validity of these results can be questioned, since measurements of the barriers to internal rotation in  $C(CH_3)_4$ ,  $Ge(CH_3)_4$ , and  $Sn(CH_3)_4$  by NMR are too low by a factor of 2 [38]. Also, other experimental measurements [41] and theoretical studies [42] suggest that there may be barriers to internal rotation about the bonds adjacent to the unpaired electron in alkyl radicals, due to a combination of effects related to hyperconjugation, spin polarization, and spin delocalization. Therefore, the internal rotations in the radicals were treated as low-frequency vibrators, hindered rotors, and free rotors in order to determine which treatment would give the best fit to estimated recombination rates. A complete description of the radical models is given in Appendix II.

#### E. Computational results for *n*-butane\*

Due to the experimental difficulty in measuring the individual contributions to *n*-butane decomposition by ethyl rupture and methyl rupture, only the total rate constant for *n*-butane decomposition was measured. Whitten and Rabino- vitch [3] studied the decomposition of  $n-C_4H_{10}^*$  formed by the reaction of  $C_3H_8$  with  $^1CH_2$ . Their singlet methylene source was the 4358-Å photolysis of diazo- methane. They found that the chemically activated *n*-butane decomposed twice as fast by ethyl rupture as by methyl rupture. This factor along with the the total decomposition rates measured in this work yield rates of ethyl rupture of  $4.9 \times 10^6$   $sec^{-1}$  and  $1.5 \times 10^7$   $sec^{-1}$  and of methyl rupture of  $2.4 \times 10^6$   $sec^{-1}$  and  $7.7 \times 10^6$   $sec^{-1}$  for the photolyses at 4358 and 3660 Å, respectively.

A description of the activated complex models that give theoretical rates in agreement with the experimental rates is given in Table III. In the  $k_{<E^*>}$  calculations for model I, the torsions in both the molecule and complex were treated as vibrations, with the frequency of the torsion about the reaction coordinate being chosen so that its entropy matched that of a free rotation. For model II, the torsions in the molecule were treated as free rotors, and the torsions in the complex were treated as vibrations. In model III, the torsions in the molecule and those in the complex adjacent to the rupturing C—C bond were treated as free rotations. The  $E_0$  values were calculated from  $D_{298}^0$  values by treating the internal rotations in the ethyl and *n*-propyl radicals as hindered rotors (see Appendix II). Though

the torsions in the molecule for models II and III were treated as free rotors in the  $k_{<E^*>}$  and calculations, they were treated as the measured hindered rotors in the calculation of the  $A$ -factors and activation energies. The torsions in the molecule are adequately approximated as free rotors for the  $k_{<E^*>}$  calculations since the level of excitation is large,  $\sim 120$  kcal/mole, but not for the thermal calculations since the average energy in the molecule is considerably reduced. It is more correct and facile to treat the torsions of the molecule as the measured hindered rotors in the thermal calculations.

The decomposition rate calculations for  $n$ -butane for the two decomposition paths are presented in Table IV. The average of the  $A$ -factors for the three models at the median  $E_0$  is  $3.4 \times 10^{16}$  sec $^{-1}$  and  $4.2 \times 10^{16}$  sec $^{-1}$  for ethyl and methyl rupture, respectively. The pyrolysis of  $n$ -butane has been studied extensively [10,11,43,44], but there has been no thermal measurement of the  $A$ -factor and activation energy for  $n$ -butane decomposition. Purnell and Quinn [43] have estimated the  $A$ -factor and activation energy for both ethyl and methyl rupture from  $n$ -butane to be identical, having values of  $3.77 \times 10^{18}$  sec $^{-1}$  and 86.3 kcal/mole, respectively. An earlier estimate by Trotman-Dickenson [45] placed the  $A$ -factor and activation energy for ethyl rupture from  $n$ -butane at  $1.0 \times 10^{17}$  sec $^{-1}$  and 80.0 kcal/mole. Recently, Tsang from his work on other alkanes calculated an  $A$ -factor and activation energy of  $10^{16.4}$  sec $^{-1}$  and 82.1 kcal/mole for ethyl rupture from  $n$ -butane [46]. The  $A$ -factors calculated here indicate that the estimates by Purnell and Quinn are too large by at least an order of magnitude. The Arrhenius parameters calculated by Tsang are in excellent agreement with our calculations. It is believed [11,44] that the initiation step in  $n$ -butane pyrolysis is the rupture of the middle C—C bond only to form two ethyl radicals, since there was no evidence for methyl rupture. These results do not contradict the factor of 2 found by Whitten and Rabinovitch for the probability of C<sub>2</sub>H<sub>5</sub> rupture versus CH<sub>3</sub> rupture, since the  $A$ -factors and activation energies in Table IV predict that only 15–20% of the initiation reaction is methyl rupture at 800°K which could easily be undetected in the pyrolysis studies.

Recombination rate calculations of C<sub>2</sub>H<sub>5</sub> + C<sub>2</sub>H<sub>5</sub> and CH<sub>3</sub> +  $n$ -C<sub>3</sub>H<sub>7</sub> using the activated complex models in Table III are given in Table V. Results are presented using tight,  $T$ , and loose,  $L$ , ethyl and  $n$ -propyl radicals (Appendix II). The entropies of the loose radicals are similar to previous estimates of the entropies of ethyl and  $n$ -propyl radicals [27,52]. The recombination rate of ethyl radicals has been measured by Shepp and Kutschke [53] to be  $2.5 \times 10^{10}$  liters mole $^{-1}$  sec $^{-1}$  at 400°K. The rate of methyl and  $n$ -propyl recombination has not been measured but was estimated here to be  $\sim 10^{10}$  liters mole $^{-1}$  sec $^{-1}$ . It is seen that model III, using the tight  $n$ -C<sub>3</sub>H<sub>7</sub> radical, gives recombination rates for CH<sub>3</sub> +  $n$ -C<sub>3</sub>H<sub>7</sub> in best agreement with the estimated rate. For ethyl recombination, the largest calculated rate is still 23 times smaller than the experimentally measured rate. This discrepancy cannot be removed by using an even tighter ethyl radical, since any further significant tightening of the ethyl radical would be completely unreasonable. Also, if it is assumed that the  $n$ -C<sub>4</sub>H<sub>10</sub>\* formed here is decomposing

TABLE III. Models for *n*-butane decomposition.

| Description of mode                      | Molecule  | Model             |      | Model  |      |
|--|---|-------------------|------|--|------|
|  |   | I                 | II   | III  | III  |
| Ethyl Rupture                            |   | $E_0 = 81.4$      |      |  |      |
| C—C Stretch                              | 835   | R.C. <sup>a</sup> | R.C. | R.C.   | R.C. |
| CH <sub>3</sub> and CH <sub>2</sub> Rock | 1152  | 302               | 202  | 270  | 219  |
| CH <sub>3</sub> Rock                     | 972   | 256               | 170  | 228  | 186  |
| C—C—C Bend                               | 431   | 113               | 76   | 101  | 82   |
| C—C—C Bend                               | 271   | 70                | 47   | 63   | 51   |
| Torsion ( $V_0 = 3.4$ ) <sup>b</sup>     | 225, F.R., F.R. <sup>c</sup>                                    | 225               | 225  | F.R.   | F.R. |
| Torsion ( $V_0 = 3.4$ )                  | 194, F.R., F.R.   | 194               | 194  | F.R.   | F.R. |
| Torsion ( $V_0 = 4.0$ )                  | 102, F.R., F.R.   | 25 <sup>d</sup>   | 25   | F.R.   | F.R. |
|  | $I_r(\text{CH}_3) = 5.1 \times 10^{-40}$ <sup>f</sup>           |                   |      | $I_r(\text{CH}_3) = 5.1 \times 10^{-40}$                               |      |
|  | $I_r(\text{CH}_3) = 5.1 \times 10^{-40}$                        |                   |      | $I_r(\text{CH}_3) = 5.1 \times 10^{-40}$                               |      |
|  | $I_r(\text{C}_2\text{H}_5) = 18.8 \times 10^{-40}$ <sup>e</sup> |                   |      | $I_r(\text{C}_2\text{H}_5) = 18.8 \times 10^{-40}$                     |      |
| Methyl Rupture                           |   | $E_0 = 83.7$      |      |  |      |
| C—C Stretch                              | 1008  | R.C. <sup>a</sup> | R.C. | R.C.   | R.C. |
| CH <sub>3</sub> and CH <sub>2</sub> Rock | 1152  | 352               | 232  | 305  | 246  |
| CH <sub>3</sub> Rock                     | 972   | 298               | 196  | 258  | 208  |
| C—C—C Bend                               | 431   | 131               | 87   | 115  | 93   |
| C—C—C Bend                               | 271   | 80                | 55   | 70   | 58   |
| Torsion ( $V_0 = 3.4$ ) <sup>b</sup>     | 225, F.R., F.R. <sup>c</sup>                                    | 225               | 225  | F.R.   | F.R. |
| Torsion ( $V_0 = 3.4$ )                  | 194, F.R., F.R.   | 50 <sup>d</sup>   | 50   | 194  | 194  |
| Torsion ( $V_0 = 4.0$ )                  | 102, F.R., F.R.   | 102               | 102  | F.R.   | F.R. |
|  | $I_r(\text{CH}_3) = 5.1 \times 10^{-40}$ <sup>f</sup>           |                   |      | $I_r(\text{CH}_3) = 5.1 \times 10^{-40}$                               |      |
|  | $I_r(\text{C}_2\text{H}_5) = 18.8 \times 10^{-40}$ <sup>e</sup> |                   |      | $I_r(\text{CH}_2-\text{CH}_3)$ <sup>g</sup> = 28.5 × 10 <sup>-40</sup> |      |

<sup>a</sup> R.C. is the reaction coordinate.

<sup>b</sup>  $V_0$  is the barrier to internal rotation as taken from refs. [47] and [48]. The barrier is in kcal/mole. Using these barriers to internal rotation, the overall rotational moments of inertia in ref. [4] ( $I_x I_y I_z \approx 2.00 \times 10^{-114}$  gr<sup>3</sup>cm<sup>6</sup>), and the vibrational frequencies in ref. [33] gives an entropy for *n*-butane of 74.3 e.u. at 298°K. The measured value is 74.12 e.u. [24].

<sup>c</sup> The first frequency listed corresponds to model I, the second to model II, and the third to model III. The torsional frequencies listed here (225, 194, 102) and the parameters in footnote *b* above give an entropy for *n*-butane of 72.5 e.u. at 298°K. This entropy is low because only one geometric isomer is considered. If both the straight and bent forms are considered [49], and the enthalpy difference between the two forms is taken as 800 cal/mole [50], the calculated entropy for *n*-butane is 74.5 e.u. at 298°K.

<sup>d</sup> This frequency was chosen to match the entropy of a free rotation.

<sup>e</sup> The reduced moment of inertia for the ethyl rotation was calculated by the method described by Herschbach and coworkers for unsymmetrical tops [51].

<sup>f</sup> The moments of inertia are in units of g-cm<sup>2</sup>.

<sup>g</sup> This is the reduced moment of the ethyl group which contains the reaction coordinate for methyl rupture.

TABLE IV. Decomposition rate calculations for *n*-butane.

| Model            | <i>A</i> -factor <sup>a</sup>              | <i>E</i> <sub>0</sub> <sup>b</sup> | <i>E</i> <sub>a</sub> <sup>a</sup> | <i>k</i> <sub>&lt;E*&gt;</sub> , sec <sup>-1</sup> |                                   |
|------------------|--|------------------------------------|------------------------------------|--|-----------------------------------|
|                  |  |                                    |                                    | <i>E</i> * = 119.7 <sup>c</sup>                    | <i>E</i> * = 123.2                |
| Ethyl Rupture    |  |                                    |                                    |  |                                   |
| I <sup>e</sup>   | 3.1 × 10 <sup>16</sup> (16.5) <sup>d</sup> | 81.4                               | 84.5                               | 6.2 × 10 <sup>6</sup>                              | 1.2 × 10 <sup>7</sup>             |
| II <sup>f</sup>  | 4.7 × 10 <sup>16</sup> (16.7)              | 81.4                               | 84.4                               | 6.1 × 10 <sup>6</sup>                              | 1.2 × 10 <sup>7</sup>             |
| III <sup>f</sup> | 2.5 × 10 <sup>16</sup> (16.4)              | 81.4                               | 82.4                               | 6.2 × 10 <sup>6</sup>                              | 1.2 × 10 <sup>7</sup>             |
|                  | 5.6 × 10 <sup>16</sup> (16.7)              | 83.4                               | 84.5                               | 6.1 × 10 <sup>6</sup>                              | 1.2 × 10 <sup>7</sup>             |
|                  |  |                                    | Experimental                       | 4.9 × 10 <sup>6</sup><br>(4358 Å)                  | 1.5 × 10 <sup>7</sup><br>(3660 Å) |
| Methyl Rupture   |  |                                    |                                    |  |                                   |
| I <sup>e</sup>   | 3.7 × 10 <sup>16</sup> (16.6)              | 83.7                               | 86.8                               | 3.0 × 10 <sup>6</sup>                              | 6.2 × 10 <sup>6</sup>             |
| II <sup>f</sup>  | 5.6 × 10 <sup>16</sup> (16.7)              | 83.7                               | 86.8                               | 2.9 × 10 <sup>6</sup>                              | 6.2 × 10 <sup>6</sup>             |
| III <sup>f</sup> | 3.4 × 10 <sup>16</sup> (16.5)              | 83.7                               | 85.2                               | 3.1 × 10 <sup>6</sup>                              | 6.2 × 10 <sup>6</sup>             |
|                  | 7.8 × 10 <sup>16</sup> (16.9)              | 85.7                               | 87.4                               | 2.9 × 10 <sup>6</sup>                              | 6.2 × 10 <sup>6</sup>             |
|                  |  |                                    | Experimental                       | 2.4 × 10 <sup>6</sup><br>(4358 Å)                  | 7.7 × 10 <sup>6</sup><br>(3660 Å) |

<sup>a</sup> The *A*-factors and Arrhenius activation energy are calculated for a temperature of 800°K. The *A*-factor is given in units of sec<sup>-1</sup> and the activation energy in kcal/mole.

<sup>b</sup> The *E*<sub>0</sub> values were calculated from the bond dissociation energies using hindered rotor ethyl and *n*-propyl radical structures.

<sup>c</sup> These energies are in kcal/mole. The heats of formation of C<sub>3</sub>H<sub>8</sub> and *n*-C<sub>4</sub>H<sub>10</sub> were taken from the A.P.I. tables. *E*<sub>thermal</sub> equals 3.0 kcal/mole.

<sup>d</sup> The log *A* values are in the parenthesis.

<sup>e</sup> The *A*-factor for model I was calculated by assuming both the molecule and complex existed in only one configuration.

<sup>f</sup> The *A*-factors for models II and III were calculated using the torsional barriers for the molecule given in Table III.

solely by C<sub>2</sub>H<sub>5</sub> rupture instead of one third by methyl rupture, the recombination rates would be only ~1.5 times larger than the recombination rates calculated here. If the external rotational degree of freedom along the "figure axis" were treated as active, as suggested by Rabinovitch and Setser [4], the rate of ethyl recombination would be only ~1.3 times larger. Therefore, there seems to be a basic discrepancy between the decomposition rates and recombinations rates for *n*-butane.

The free-rotor activated complex model gives the best correlation between the decomposition and recombination rates for both reaction paths. It is emphasized that treating the torsions in the molecule as free rotors for the *k*<sub><E\*></sub> calculations gives larger *A*-factors and recombination rates. This treatment seems the most appropriate since the resulting activated complexes give larger recombination

TABLE V. Recombination rate calculations for *n*-butane.<sup>a,d</sup>

| Model          | $E_0$        | $k_r(T)^b$             | $k_r(L)^c$           |
|----------------|--------------|------------------------|----------------------|
| Ethyl Rupture  |              |                        |                      |
| I <sup>e</sup> | 81.4         | $1.2 \times 10^8$      | $8.5 \times 10^7$    |
| II             | 81.4         | $1.4 \times 10^8$      | $9.5 \times 10^7$    |
| III            | 81.4         | $5.7 \times 10^8$      | $3.8 \times 10^8$    |
|                | 83.4         | $1.1 \times 10^9$      | $7.2 \times 10^8$    |
|                | Experimental | $2.5 \times 10^{10} f$ | $2.5 \times 10^{10}$ |
| Methyl Rupture |              |                        |                      |
| I <sup>e</sup> | 83.7         | $9.1 \times 10^8$      | $3.7 \times 10^8$    |
| II             | 83.7         | $9.5 \times 10^8$      | $3.8 \times 10^8$    |
| III            | 83.7         | $3.1 \times 10^9$      | $1.3 \times 10^9$    |
|                | 85.7         | $5.7 \times 10^9$      | $2.3 \times 10^9$    |
|                | Experimental | $\sim 10^{10} f$       | $\sim 10^{10}$       |

<sup>a</sup> The recombination rates were calculated at 400°K.

<sup>b</sup> These recombination rates were calculated using the tight radicals.

<sup>c</sup> These recombination rates were calculated using the loose radicals.

<sup>d</sup> The calculated entropy of *n*-butane at 400°K is 82.0 e.u. if the torsions are treated as hindered rotors (Table III) and the other parameters are the same as those given in Table III, footnote *b*. This entropy was used for models II and III. The measured entropy at 400°K is 81.86 e.u. [60]. The overall rotational and translational entropy for *n*-butane at 400°K is 63.55 e.u. using the moments of inertia given in ref. [4]. The average overall rotational and translational entropy of the bent and straight forms of *n*-butane is 64.49 e.u. If this entropy value (64.49) had been used, the  $k_r$  values for models II and III would be 1.54 times larger.

<sup>e</sup> In calculating the recombination rates for model I, both the bent and straight configurations were included in calculating the entropy of the complex (Table III, footnote *c*), so that the rates could be compared with experiment. The calculated entropy of the vibrator molecule at 400°K is 82.09 e.u. If the torsions in the molecule had been treated as vibrators with frequencies giving the measured entropy, the recombination rates would be 1.12 times lower.

<sup>f</sup> The  $C_2H_5 + C_2H_5$  recombination rate was taken from ref. [53], and the  $CH_3 + n-C_3H_7$  was estimated.

rates than the recombination rates calculated using activated complexes derived from the  $k_{<E^*>}$  calculations by treating the torsions in the molecule as vibrations.

#### F. Calculational results for isopentane\* and neohexane\*

There have been no thermal measurements of the Arrhenius parameters for either isopentane\* or neohexane\* decomposition, and there have been no previous chemical activation studies of isopentane\* or neohexane\* decomposition which would provide information about the relative probabilities for decomposition by the various possible paths. Therefore, the structures for the appropriate activated complexes were assumed to be similar to previous isobutane [5,6], neopentane [5,6], and *n*-butane complex models for nearly identical reaction paths. Only the free-rotor complex models were used for these initial calculations. In the acti-

vated complex model for isopentane\* decomposition into  $\text{CH}_3$  and  $i\text{-C}_4\text{H}_9$  radicals, two  $\text{CH}_3$  rocking and two C—C—C bending motions were lowered by the same factor (3.80), as they were for  $\text{CH}_3$  rupture from  $n\text{-C}_4\text{H}_{10}^*$  at the same  $E_0$ . In the activated complex leading to formation of  $\text{CH}_3$  and  $sec\text{-C}_4\text{H}_9$  radicals, two  $\text{CH}_3$  rocking and two C—C—C bending motions were lowered by the same factor, 4.05, as they were for  $i\text{-C}_4\text{H}_{10}^*$  decomposition at the same  $E_0$  [5,6]. For ethyl rupture from isopentane\*, one  $\text{CH}_2$  rocking and three C—C—C bending motions were lowered in the activated complex by a factor of  $4.05 \times 4.26/3.80$ , the same lowering as for  $\text{CH}_3$  rupture from  $i\text{-C}_4\text{H}_{10}^*$  [5,6] times the ratio of factors for ethyl-versus-methyl rupture from  $n\text{-C}_4\text{H}_{10}^*$ ; i.e., a total factor of 4.56.

Frequencies were lowered in the activated complexes for the three neohexane decomposition paths in a similar fashion. In the activated complex model giving  $\text{CH}_3$  and  $neo\text{-C}_5\text{H}_{11}$  radicals, two  $\text{CH}_3$  rocking and two C—C—C bending motions were lowered by the same factor, 3.80, as they were for  $\text{CH}_3$  rupture from  $n\text{-C}_4\text{H}_{10}^*$  at the same  $E_0$ . For the activated complex leading to the formation of  $\text{CH}_3$  and  $t\text{-C}_5\text{H}_{11}$  radicals, two  $\text{CH}_3$  rocking and two C—C—C bending motions were lowered by the same factor (4.45) as they were for  $neo\text{-C}_5\text{H}_{12}^*$  decomposition at the same  $E_0$  [5,6]. For ethyl rupture from neohexane, one  $\text{CH}_2$  rocking and three C—C—C bending motions were lowered in the activated complex by a factor of  $4.45 \times 4.26/3.80 = 5.00$ , the same lowering as for  $\text{CH}_3$  rupture from  $neo\text{-C}_5\text{H}_{12}^*$  [5,6] times the ratio of factors for ethyl-versus-methyl rupture from  $n\text{-C}_4\text{H}_{10}^*$ . The  $E_0$  values were calculated using the tight radical structures (Appendix II). A complete description of these models is presented in Table VI.

The calculational results using these activated complex models are given in Table VII. The torsions in the molecules were treated as free rotors in the  $k_{<E^*>}$  calculations. The  $N(\langle E_{\ddot{V}R}^* \rangle)$  values would be 6.1 and 3.1 times lower if the torsions were treated as the corresponding vibrators for isopentane and neohexane, respectively. Although the total calculated isopentane decomposition rates are slightly low for the three smallest  $E^*$  values, they are still in satisfactory agreement with the experimental rates. For neohexane, the calculated rates are only 1.3 times lower than the experimental rates. The recombination rates for these radicals were estimated as  $\sim 10^{10}$  liters mole $^{-1}$  sec $^{-1}$ . The calculated recombination rates, using tight radical structures, are in approximate agreement with this estimate, except for the rate of  $\text{CH}_3 + neo\text{-C}_5\text{H}_{11}$  which is a factor of 4.0 too small. The calculated  $k_{<E^*>}$  values and the recombination rates could be brought into better agreement with the overall experimental decomposition rates and estimated recombination rates, if the vibrational frequencies in the complex models were lowered slightly from those given in Table VI.

A significant result from these calculations is that activated complex models deduced a priori from similar decomposition paths for isobutane, neopentane, and  $n$ -butane gave overall decomposition rates in good agreement with the experimental rates for isopentane and neohexane decompositions.

In order to determine if vibrator complex models would give recombination rates in agreement with the estimated rates in these cases, vibrator complex models

TABLE VI. Free-rotor complex models for isopentane and neohexane decomposition based on neopentane, isobutane, and *n*-butane complex models.

| Isopentane frequencies, $\text{cm}^{-1}$ <sup>a</sup>               |                             |  |                             |  |                             |  |  |  |  |  |  |
|---|-----------------------------|--|-----------------------------|--|-----------------------------|--|--|--|--|--|--|
| Isopentane $\longrightarrow$ $\text{CH}_3 + i\text{-C}_4\text{H}_9$ |                             | Isopentane $\longrightarrow$ $\text{CH}_3 + \textit{sec}\text{-C}_4\text{H}_9$ |                             | Isopentane $\longrightarrow$ $\text{C}_2\text{H}_5 + i\text{-C}_3\text{H}_7$ |                             |  |  |  |  |  |  |
| Motion  | Molecule                    | Motion   | Molecule                    | Motion   | Molecule                    |  |  |  |  |  |  |
| C—C Stretch   | 1039                        | C—C Stretch  | 901                         | C—C Stretch  | 793                         |  |  |  |  |  |  |
| $\text{CH}_3$ Rock  | 1168                        | $\text{CH}_3$ Rock   | 974                         | $\text{CH}_2 + \text{CH}_3$ Rock   | 768                         |  |  |  |  |  |  |
| $\text{CH}_2 + \text{CH}_3$ Rock                                    | 768                         | $\text{CH}_3$ Rock   | 958                         | C—C—C Bend   | 412                         |  |  |  |  |  |  |
| C—C—C Bend  | 461                         | C—C—C Bend   | 412                         | C—C—C Bend   | 365                         |  |  |  |  |  |  |
| C—C—C Bend  | 260                         | C—C—C Bend   | 365                         | C—C—C Bend   | 260                         |  |  |  |  |  |  |
| Torsion (4.0) <sup>f</sup>  | F.R. (204) <sup>b</sup>     | Torsion  | F.R. (204)                  | Torsion  | F.R. (204)                  |  |  |  |  |  |  |
| Torsion (4.0)   | F.R. (198)                  | Torsion  | F.R. (198)                  | Torsion  | F.R. (198)                  |  |  |  |  |  |  |
| Torsion (4.0)   | F.R. (193)                  | Torsion  | F.R. (193)                  | Torsion  | F.R. (193)                  |  |  |  |  |  |  |
| Torsion (4.0)   | F.R. (84)                   | Torsion  | F.R. (84)                   | Torsion  | F.R. (84)                   |  |  |  |  |  |  |
|   | $I_r(\text{C}_2\text{H}_5)$ |  | $I_r(\text{C}_2\text{H}_5)$ |  | $I_r(\text{C}_2\text{H}_5)$ |  |  |  |  |  |  |
|   | $26.5 \times 10^{-40c}$     |  | $32.6 \times 10^{-40}$      |  | $26.5 \times 10^{-40}$      |  |  |  |  |  |  |
|   | $50.8 \times 10^{-40}$      |  |                             |  |                             |  |  |  |  |  |  |

| Neohexane frequencies, cm <sup>-1</sup> <sup>a</sup>             |   |  |   |   |   |
|--|---|--|---|---|---|
| Neohexane → CH <sub>3</sub> + neo-C <sub>3</sub> H <sub>11</sub> |   | Neohexane → CH <sub>3</sub> + <i>t</i> -C <sub>3</sub> H <sub>11</sub> |   | Neohexane → C <sub>2</sub> H <sub>5</sub> + <i>t</i> -C <sub>4</sub> H <sub>9</sub> |   |
| Motion   | Molecule  | Motion   | Molecule  | Motion  | Molecule  |
| Complex  |   | Complex  |   | Complex   |   |
| C—C Stretch  | 1027  | C—C Stretch  | 921   | C—C Stretch   | 714   |
| CH <sub>3</sub> + CH <sub>2</sub> Rock                           | 1099  | CH <sub>3</sub> Rock   | 981   | CH <sub>3</sub> + CH <sub>2</sub> Rock  | 790   |
| CH <sub>3</sub> + CH <sub>2</sub> Rock                           | 790   | CH <sub>3</sub> Rock   | 866   | C—C—C Bend  | 394   |
| C—C—C Bend   | 394   | C—C—C Bend   | 356   | C—C—C Bend  | 356   |
| C—C—C Bend   | 232   | C—C—C Bend   | 351   | C—C—C Bend  | 232   |
| Torsion (4.0) <sup>e</sup>                                       | F.R. (201)  | Torsion  | F.R. (201)  | Torsion   | F.R. (201)  |
| Torsion (4.0)  | F.R. (197)  | Torsion  | F.R. (197)  | Torsion   | F.R. (197)  |
| Torsion (4.0)  | F.R. (197)  | Torsion  | F.R. (197)  | Torsion   | F.R. (197)  |
| Torsion (4.0)  | F.R. (193)  | Torsion  | F.R. (193)  | Torsion   | F.R. (193)  |
| Torsion (4.0)  | F.R. (76)   | Torsion  | F.R. (76)   | Torsion   | F.R. (76)   |
|  | <i>I<sub>r</sub></i> (C <sub>2</sub> H <sub>6</sub> ) |  | <i>I<sub>r</sub></i> (C <sub>2</sub> H <sub>6</sub> ) |   | <i>I<sub>r</sub></i> (C <sub>2</sub> H <sub>6</sub> ) |
|  | 32.0 × 10 <sup>-40e</sup>                             |  | 76.1 × 10 <sup>-40</sup>                              |   | 32.0 × 10 <sup>-40</sup>                              |

<sup>a</sup> *I<sup>+</sup>/I* equals 4.0 for all the models. The frequencies were taken from ref. [34].  
<sup>b</sup> The reduced moments of inertia of all the methyl rotations in the isopentane molecule and complexes are  $5.3 \times 10^{-40}$  g-cm<sup>2</sup>. In parenthesis is the frequency for which the torsion was treated in the  $N(E_{VR}^*)$  calculations for the vibrator molecule model. F.R. = free rotor.  
<sup>c</sup> This moment of inertia is in units of g-cm<sup>2</sup>. The values for *I<sub>r</sub>*(C<sub>2</sub>H<sub>6</sub>) were calculated by the method described by Herschbach et al. [51].  
<sup>d</sup> The reduced moments of inertia of all the methyl internal rotations in the neohexane molecule and complexes are  $5.3 \times 10^{-40}$  g-cm<sup>2</sup>. In parenthesis is the frequency for which the torsion was treated in the  $N(E_{VR}^*)$  calculations for the vibrator molecule model. F.R. = free rotor.  
<sup>e</sup> R.C. = reaction coordinate.  
<sup>f</sup> In the parentheses are the barriers to internal rotation for the torsions. The torsions were treated as these hindered rotors for the molecule in the thermal Arrhenius parameter calculations. The calculated entropy for isopentane at 298°K is 81.96 e.u. using these barriers to internal rotation, the isopentane frequencies of ref. [34], and *I<sub>x</sub>I<sub>y</sub>I<sub>z</sub>* =  $9.75 \times 10^{-14}$  g<sup>3</sup>-cm<sup>6</sup> (where the tertiary H and two carbons of the ethyl group lie in a plane). The measured value is 82.12 e.u. [24].  
<sup>g</sup> In the parentheses are the barriers to internal rotation for the torsions. The torsions in the molecule were treated as these hindered rotors in the thermal Arrhenius parameter calculations. The calculated entropy for neohexane at 298°K is 85.74 e.u. using these barriers to internal rotation, the neohexane frequencies of ref. [34], and the translation and overall rotation entropy from ref. [54]. The measured entropy is 85.72 e.u. [24]. *I<sub>x</sub>I<sub>y</sub>I<sub>z</sub>* =  $20.31 \times 10^{-14}$  g<sup>3</sup>-cm<sup>6</sup> for neohexane.

TABLE VII. Calculations for isopentane and neohexane using free rotor-activated complex complex models like those for neopentane, isobutane, and *n*-butane<sup>a</sup>

| Isopentane calculations <sup>d</sup>                                    |                               |                       |                                    |   |                        |                        |                                       |                       |
|---|-------------------------------|-----------------------|------------------------------------|---|------------------------|------------------------|---------------------------------------|-----------------------|
| Reaction path   | <i>A</i> -factor              | <i>E</i> <sub>0</sub> | <i>E</i> <sub>a</sub> <sup>b</sup> | <i>k</i> <sub>&lt;E*⟩</sub> , sec <sup>-1</sup> |                        |                        | <i>k<sub>r</sub></i> (T) <sup>c</sup> |                       |
|   |                               |                       |                                    | <i>E</i> * = 119.9                              | <i>E</i> * = 121.5     | <i>E</i> * = 123.4     |                                       | <i>E</i> * = 125.0    |
| CH <sub>3</sub> + <i>i</i> -C <sub>4</sub> H <sub>9</sub>               | 3.5 × 10 <sup>16</sup>        | 83.6                  | 85.0                               | 0.03 × 10 <sup>6</sup>                          | 0.04 × 10 <sup>6</sup> | 0.07 × 10 <sup>6</sup> | 0.09 × 10 <sup>6</sup>                | 3.8 × 10 <sup>9</sup> |
| CH <sub>3</sub> + <i>sec</i> -C <sub>4</sub> H <sub>9</sub>             | 7.9 × 10 <sup>16</sup>        | 81.4                  | 82.1                               | 0.24 × 10 <sup>6</sup>                          | 0.33 × 10 <sup>6</sup> | 0.50 × 10 <sup>6</sup> | 0.68 × 10 <sup>6</sup>                | 4.3 × 10 <sup>9</sup> |
| C <sub>2</sub> H <sub>5</sub> + <i>i</i> -C <sub>3</sub> H <sub>7</sub> | 6.5 × 10 <sup>16</sup>        | 79.3                  | 78.7                               | 0.88 × 10 <sup>6</sup>                          | 1.17 × 10 <sup>6</sup> | 1.71 × 10 <sup>6</sup> | 2.24 × 10 <sup>6</sup>                | 6.3 × 10 <sup>9</sup> |
|   |                               |                       | Total <i>k</i> <sub>&lt;E*⟩</sub>  | 1.15 × 10 <sup>6</sup>                          | 1.54 × 10 <sup>6</sup> | 2.28 × 10 <sup>6</sup> | 3.01 × 10 <sup>6</sup>                |                       |
|   |                               |                       | Experimental                       | 1.6 × 10 <sup>6</sup>                           | 2.2 × 10 <sup>6</sup>  | 3.1 × 10 <sup>6</sup>  | 2.8 × 10 <sup>6</sup>                 |                       |
| Neohexane calculations <sup>d</sup>                                     |                               |                       |                                    |   |                        |                        |                                       |                       |
| Reaction path   | <i>A</i> -factor <sup>b</sup> | <i>E</i> <sub>0</sub> | <i>E</i> <sup>a,b</sup>            | <i>k</i> <sub>&lt;E*⟩</sub> , sec <sup>-1</sup> |                        |                        | <i>k<sub>r</sub></i> (T) <sup>c</sup> |                       |
|   |                               |                       |                                    | <i>E</i> * = 120.6                              | <i>E</i> * = 124.1     | <i>E</i> * = 124.1     |                                       |                       |
| CH <sub>3</sub> + neo-C <sub>5</sub> H <sub>11</sub>                    | 2.6 × 10 <sup>16</sup>        | 83.6                  | 85.0                               | 0.01 × 10 <sup>5</sup>                          | 0.02 × 10 <sup>5</sup> | 0.02 × 10 <sup>5</sup> | 2.5 × 10 <sup>9</sup>                 |                       |
| CH <sub>3</sub> + <i>t</i> -C <sub>5</sub> H <sub>11</sub>              | 1.4 × 10 <sup>17</sup>        | 78.4                  | 78.5                               | 0.94 × 10 <sup>5</sup>                          | 1.97 × 10 <sup>5</sup> | 1.97 × 10 <sup>5</sup> | 1.1 × 10 <sup>10</sup>                |                       |
| C <sub>2</sub> H <sub>5</sub> + <i>t</i> -C <sub>4</sub> H <sub>9</sub> | 6.9 × 10 <sup>16</sup>        | 76.1                  | 74.8                               | 2.59 × 10 <sup>5</sup>                          | 5.04 × 10 <sup>5</sup> | 5.04 × 10 <sup>5</sup> | 7.6 × 10 <sup>9</sup>                 |                       |
|   |                               |                       | Total <i>k</i> <sub>&lt;E*⟩</sub>  | 3.54 × 10 <sup>5</sup>                          | 7.03 × 10 <sup>5</sup> | 7.03 × 10 <sup>5</sup> |                                       |                       |
|   |                               |                       | Experimental                       | 4.6 × 10 <sup>5</sup>                           | 8.7 × 10 <sup>5</sup>  | 8.7 × 10 <sup>5</sup>  |                                       |                       |

<sup>a</sup> All energies are in kcal/mole.

<sup>b</sup> The *A*-factors and activation energies were calculated for a temperature of 1000°K.

<sup>c</sup> The recombination rates were calculated for a temperature of 400°K using tight radical structures.

<sup>d</sup> *E*<sub>1/8</sub> equals 3.8 kcal/mole for isopentane\* and 4.6 kcal/mole for neohexane\*. The heats of formation of *n*-butane, isobutane, neopentane, and neohexane were taken from the A.P.I. tables [24].

were chosen which gave values of  $k_{<E^*>}$  identical to those calculated for the free-rotor models. The same activated complex frequencies were lowered as before (Table VI), and the torsional frequencies along the reaction coordinates were chosen so that their entropies matched those of the corresponding free rotors. A description of the vibrator models is given in Table VIII.  $A$ -factors and recombination rates calculated for the vibrator models are presented in Table IX. The recombination rates calculated using vibrator complex models and loose radicals are all lower than those calculated for the free-rotor complex models.

The  $A$ -factors calculated for  $\text{CH}_3$  rupture from isopentane and neohexane using the free-rotor complex models (Table VII) are all about  $4 \times 10^{16} \text{ sec}^{-1}$  for the cleavage of a particular type of C—C bond. The  $A$ -factors for ethyl rupture are slightly larger,  $6.5 \times 10^{16} \text{ sec}^{-1}$  and  $6.9 \times 10^{16} \text{ sec}^{-1}$  for isopentane and neohexane, respectively. For the vibrator complex models, the  $A$ -factors are 3–4 times larger than those calculated for the free-rotor complex models (Table IX)

TABLE VIII. Vibrator complex models for isopentane and neohexane decomposition.

| Isopentane Vibrator Complex Models <sup>a</sup> Frequencies, $\text{cm}^{-1}$ |   |   |
|---|---|---|
| $\text{CH}_3 + i\text{-C}_4\text{H}_9$  | $\text{CH}_3 + \text{sec-C}_4\text{H}_9$  | $\text{C}_2\text{H}_5 + i\text{-C}_3\text{H}_7$ |
| 230   | 170                                       | 112   |
| 151   | 167                                       | 60  |
| 91  | 71  | 53  |
| 51  | 63  | 38  |
| 204   | 51 <sup>b</sup>                           | 204   |
| 198   | 198                                       | 198   |
| 48 <sup>b</sup>   | 193                                       | 193   |
| 84  | 84  | 21 <sup>b</sup>                                 |
| Neohexane Vibrator Complex Models <sup>a</sup> Frequencies, $\text{cm}^{-1}$  |   |   |
| $\text{CH}_3 + \text{neo-C}_5\text{H}_{11}$                                   | $\text{CH}_3 + t\text{-C}_5\text{H}_{11}$ | $\text{C}_2\text{H}_5 + t\text{-C}_4\text{H}_9$ |
| 276   | 176                                       | 118   |
| 195   | 161                                       | 59  |
| 99  | 67  | 53  |
| 58  | 66  | 35  |
| 201   | 50 <sup>b</sup>                           | 201   |
| 197   | 197                                       | 197   |
| 197   | 197                                       | 197   |
| 48 <sup>b</sup>   | 193                                       | 193   |
| 76  | 76  | 19 <sup>b</sup>                                 |

<sup>a</sup> The same frequencies were adjusted as in Table VI. The frequencies are expressed in units of  $\text{cm}^{-1}$ .

<sup>b</sup> This frequency was chosen so that its entropy matched that of a free rotor.

TABLE IX. Calculations for the isopentane and neohexane vibrator complex models<sup>a</sup>

| Reaction path                                   | $A$ -factor <sup>b</sup> | $E_0$ | $E_a^b$ | $k_r(T)^c$        |
|---|--------------------------|-------|---------|-------------------|
| Isopentane Vibrator Models                      |                          |       |         |                   |
| $\text{CH}_3 + i\text{-C}_4\text{H}_9$          | $8.7 \times 10^{16}$     | 83.6  | 87.0    | $1.4 \times 10^9$ |
| $\text{CH}_3 + \text{sec-C}_4\text{H}_9$        | $2.4 \times 10^{17}$     | 81.4  | 84.9    | $1.1 \times 10^9$ |
| $\text{C}_2\text{H}_5 + i\text{-C}_3\text{H}_7$ | $2.4 \times 10^{17}$     | 79.3  | 82.0    | $1.1 \times 10^9$ |
| Neohexane Vibrator Models                       |                          |       |         |                   |
| $\text{CH}_3 + \text{neo-C}_5\text{H}_{11}$     | $6.3 \times 10^{16}$     | 83.6  | 86.5    | $1.1 \times 10^9$ |
| $\text{CH}_3 + t\text{-C}_5\text{H}_{11}$       | $6.7 \times 10^{17}$     | 78.4  | 81.8    | $2.5 \times 10^9$ |
| $\text{C}_2\text{H}_5 + t\text{-C}_4\text{H}_9$ | $4.4 \times 10^{17}$     | 76.1  | 78.8    | $1.3 \times 10^9$ |

<sup>a</sup> All energies are in kcal/mole.

<sup>b</sup> The  $A$ -factors and activation energies were calculated for a temperature of 1000°K.

<sup>c</sup> The recombination rates were calculated for a temperature of 400°K. using tight radical structures. They are expressed in units of liters mole<sup>-1</sup> sec<sup>-1</sup>.

Leathard and Purnell [55] have estimated the  $A$ -factor and activation energy for ethyl rupture from isopentane to be  $10^{16.8}$  sec<sup>-1</sup> and 77.3 kcal/mole, respectively. These values are in excellent agreement with the  $A$ -factor and activation energy calculated here,  $10^{16.8}$  sec<sup>-1</sup> and 78.7 kcal/mole, using the free-rotor complex model (Table VII). From the results of his shock tube studies of other alkanes, Tsang [46] places the  $A$ -factor and activation energy for ethyl rupture from isopentane and neohexane at  $10^{16.3}$  sec<sup>-1</sup> and 77.7 kcal/mole and  $10^{16.2}$  sec<sup>-1</sup> and 77.7 kcal/mole, respectively. These rate parameters are in reasonable agreement with those calculated here using free rotor-activated complex models.

#### G. Computational results for *n*-pentane\*

The activated complexes for *n*-pentane decomposition were assumed to be similar to those for *n*-butane decomposition. For methyl rupture from *n*-pentane, two methyl rocking and two C—C—C bending motions were lowered by a factor of 3.8; and for ethyl rupture, two CH<sub>2</sub> rocking and two C—C—C bending motions were lowered by a factor of 4.26. These frequency lowerings are the same as in the activated complexes for methyl and ethyl rupture from *n*-C<sub>4</sub>H<sub>10</sub>\* at the same values of  $E_0$ . A description of the activated complex models is given in Table X. Three different treatments of the torsion modes in the *n*-pentane molecule were used. In the first treatment, I, the four torsions were treated as free rotors; in the second treatment, II, three torsions were treated as free rotors and the one ethyl torsion was treated as a vibration with a frequency as in the *n*-pentane molecule; and in the third treatment, III, the four torsions were treated as the appropriate measured vibrations. The calculated results using these models are given in Table X. It is seen that treating one ethyl internal rotation as a vibrator and the remaining three internal rotations in the molecule as free rotors (treatment II) gives calculated values of  $k_{<E^*>}$  in considerably better agreement with the experimental values than either of treatments I or III. These results indicate, if these complex models are appropriate for *n*-pentane decomposition, that at this level of

excitation (120.0–123.5 kcal/mole) both ethyl internal rotations in the  $n\text{-C}_6\text{H}_{12}^*$  molecule cannot be satisfactorily treated as free rotors, but a reasonable treatment results by taking one as a free rotor and one as the measured  $95\text{-cm}^{-1}$  vibrator. This result can be compared to those found for isopentane and neohexane. For isopentane, which has 3 methyl internal rotations and 1 ethyl internal rotation, activated complexes similar to those for isobutane, which has 3 methyl internal rotations, gave values of  $k_{<E^*>}$  in good agreement with the experimental values by treating the four torsions in isopentane as free rotors. Activated complexes similar to those for neopentane, which has 4 methyl internal rotations, gave calculated values of  $k_{<E^*>}$  for neohexane, which has 4 methyl and 1 ethyl internal rotations, in good agreement with the experimental values when all the torsions in  $\text{neo-C}_6\text{H}_{14}^*$  were treated as free rotors. Thus, it seems that it is necessary to treat 1 ethyl internal rotation in a molecule as a free rotor at this level of excitation but that it is unsatisfactory to treat 2 ethyl rotations in the molecule as free rotors.

The calculated  $k_{<E^*>}$  values in Table X for ethyl rupture are 20 times larger than the values calculated for methyl rupture. This factor is significantly different than the factor of 4 one would predict from the results of Whitten and Rabinovitch [3] for  $n$ -butane decomposition (the factor of 4 includes the ratio of reaction path degeneracies for ethyl rupture from  $n$ -pentane versus ethyl rupture from  $n$ -butane). This difference in probabilities of ethyl rupture is due to the additional internal degrees of freedom in  $n$ -pentane which decrease the probability of energy amounts above the critical energy flowing to the reaction coordinates and therefore increases the probability of decomposition by the path with the lowest critical energy.

The calculated recombination rates for  $\text{CH}_3 + n\text{-C}_4\text{H}_9$  and  $\text{C}_2\text{H}_5 + n\text{-C}_3\text{H}_7$  are 12.8 and 4.6 times smaller, respectively, than our estimate of the recombination rates of  $\sim 10^{10}$  liters mole $^{-1}$  sec $^{-1}$ . The recombination rate for  $\text{CH}_3 + n\text{-C}_4\text{H}_9$  could be brought into better agreement by slight adjustments in the complex model. One constraint in these adjustments is that the resultant probability of ethyl-to-methyl rupture should be greater than 4.

#### H. Discussion of the alkane calculations

A summary of the alkane calculational results that give the best agreement with the bond dissociation energies, the estimated experimental recombination rates, and the chemical activation decomposition rates is presented in Table XI. The  $E_0$  values were calculated from the mean bond dissociation energies (Table II) using tight radical structures. Since  $E_0$  should be independent of the complex model, identical  $E_0$  values are used for both the vibrator and free-rotor complex models for the same reaction path in Table XI. The vibrator complex models for methyl and ethyl ruptures from  $n$ -pentane were chosen so that they gave the same  $k_{<E^*>}$  values as the free-rotor complex models. Except for isobutane and neopentane, for which the calculations have been described previously [5,6], the remaining parameters listed in Table XI were calculated using the complex structures described in the text.

TABLE X. *n*-Pentane calculations for complexes derived from *n*-butane complex models.<sup>a</sup>

| Reaction path  | <i>A</i> -factor <sup>b</sup> | <i>E</i> <sub>0</sub> | <i>E</i> <sub>0</sub> <sup>b</sup> | <i>k</i> <sub>&lt;<i>E</i><sup>*</sup>&gt;</sub> , sec <sup>-1</sup> |                        |                        |                               |                        |                         |
|--|-------------------------------|-----------------------|------------------------------------|--|------------------------|------------------------|-------------------------------|------------------------|-------------------------|
|  |                               |                       |                                    | <i>E</i> <sup>*</sup> = 120.0  |                        |                        | <i>E</i> <sup>*</sup> = 123.5 |                        |                         |
|  |                               |                       |                                    | I  | II                     | III                    | I                             | II                     | III                     |
| CH <sub>3</sub> Rupture                                | 1.2 × 10 <sup>16</sup>        | 83.7                  | 85.4                               | 0.01 × 10 <sup>6</sup>   | 0.06 × 10 <sup>6</sup> | 0.28 × 10 <sup>6</sup> | 0.03 × 10 <sup>6</sup>        | 0.11 × 10 <sup>6</sup> | 0.60 × 10 <sup>6</sup>  |
| C <sub>2</sub> H <sub>5</sub> Rupture                  | 5.3 × 10 <sup>16</sup>        | 81.5                  | 81.9                               | 0.32 × 10 <sup>6</sup>   | 1.23 × 10 <sup>6</sup> | 6.08 × 10 <sup>6</sup> | 0.66 × 10 <sup>6</sup>        | 2.53 × 10 <sup>6</sup> | 12.20 × 10 <sup>6</sup> |
| Total <i>k</i> <sub>&lt;<i>E</i><sup>*</sup>&gt;</sub> |                               |                       |                                    | 0.33 × 10 <sup>6</sup>   | 1.29 × 10 <sup>6</sup> | 6.36 × 10 <sup>6</sup> | 0.69 × 10 <sup>6</sup>        | 2.64 × 10 <sup>6</sup> | 12.80 × 10 <sup>6</sup> |
| Experimental   |                               |                       |                                    |  | 1.5 × 10 <sup>6</sup>  |                        |                               | 1.85 × 10 <sup>6</sup> |                         |

| Recombination Rates   |                   | Complex Models <sup>d, e</sup> |                 |                         |                 |                                       |  |
|---|-------------------|--------------------------------|-----------------|-------------------------|-----------------|---------------------------------------|--|
|   |                   | $k_r(T)^c$                     | $D_{298}^0$     | CH <sub>3</sub> Rupture |                 | C <sub>2</sub> H <sub>5</sub> Rupture |  |
| Reaction  |                   |                                | Molecule        | Complex                 | Molecule        | Complex                               |  |
| CH <sub>3</sub> + <i>n</i> -C <sub>4</sub> H <sub>9</sub>               | $7.8 \times 10^8$ | 85.0                           | 1026            | R.C.                    | 842             | R.C.                                  |  |
| C <sub>2</sub> H <sub>5</sub> + <i>n</i> -C <sub>3</sub> H <sub>7</sub> | $2.2 \times 10^9$ | 82.0                           | 1053            | 278                     | 762             | 178                                   |  |
|   |                   |                                | 926             | 243                     | 725             | 170                                   |  |
|   |                   |                                | 725             | 191                     | 491             | 115                                   |  |
|   |                   |                                | 355             | 93                      | 355             | 83                                    |  |
|   |                   |                                | I II III        |                         | I II III        |                                       |  |
|   |                   |                                | F.R., F.R., 211 | 211                     | F.R., F.R., 211 | 211                                   |  |
|   |                   |                                | F.R., F.R., 188 | F.R.                    | F.R., F.R., 188 | F.R.                                  |  |
|   |                   |                                | F.R., 95, 95    | 95                      | F.R., 95, 95    | F.R.                                  |  |
|   |                   |                                | F.R., F.R., 82  | F.R.                    | F.R., F.R., 82  | F.R.                                  |  |

<sup>a</sup> All energies are in kcal/mole.  $E_{1A}$  equals 3.8 kcal/mole for *n*-pentane\*.

<sup>b</sup> The *A*-factors and activation energies were calculated for a temperature of 1000°K.

<sup>c</sup> The recombination rates were calculated at 400°K using tight radical structures. They are expressed in liters mole<sup>-1</sup> sec<sup>-1</sup>.

<sup>d</sup> The adjusted frequencies are CH<sub>3</sub> and CH<sub>2</sub> rocking and C—C—C bending motions [34]. The frequencies are in cm<sup>-1</sup>.

<sup>e</sup> In the thermal Arrhenius calculations the ethyl and methyl rotors were treated as the appropriate hindered rotors. The barriers to internal rotation for the ethyl rotors and methyl rotors were assumed to be 4.0 and 3.4 kcal/mole, respectively. The calculated entropy for *n*-pentane at 298°K is 83.35 e.u. The measured value is 83.40 e.u. [24]. The vibrational frequencies were taken from ref. [34] and  $I_e I_e I_e$  equals  $99.5 \times 10^{-144} \text{ g}^3 \text{ cm}^6$  for the straight-planar *n*-pentane configuration.

TABLE XI. Summary of alkane calculations.<sup>a, b, c</sup>

| Reaction  | Model | $A$ -factor          | $E_0$ | $E_a$ | $k_r(T)^d$           | $k_r(L)^e$        |
|---|-------|----------------------|-------|-------|----------------------|-------------------|
| CH <sub>3</sub> + <i>i</i> -C <sub>3</sub> H <sub>7</sub>               | F.R.  | $6.4 \times 10^{16}$ | 81.4  | 82.6  | $3.3 \times 10^9$    | $1.8 \times 10^9$ |
|   | vib.  | $9.2 \times 10^{16}$ | 81.4  | 84.1  | $9.1 \times 10^8$    | $4.9 \times 10^8$ |
| CH <sub>3</sub> + <i>t</i> -C <sub>4</sub> H <sub>9</sub>               | F.R.  | $1.4 \times 10^{17}$ | 78.4  | 78.5  | $5.0 \times 10^9$    | $1.9 \times 10^9$ |
|   | vib.  | $5.1 \times 10^{17}$ | 78.4  | 81.2  | $9.9 \times 10^8$    | $4.0 \times 10^8$ |
| C <sub>2</sub> H <sub>5</sub> + C <sub>2</sub> H <sub>5</sub>           | F.R.  | $2.5 \times 10^{16}$ | 81.4  | 82.4  | $5.7 \times 10^8$    | $3.8 \times 10^8$ |
|   | vib.  | $4.7 \times 10^{16}$ | 81.4  | 84.4  | $1.4 \times 10^8$    | $9.5 \times 10^7$ |
| CH <sub>3</sub> + <i>n</i> -C <sub>3</sub> H <sub>7</sub>               | F.R.  | $3.4 \times 10^{16}$ | 83.7  | 85.2  | $3.1 \times 10^9$    | $1.3 \times 10^9$ |
|   | vib.  | $5.6 \times 10^{16}$ | 83.7  | 86.8  | $9.5 \times 10^8$    | $3.8 \times 10^8$ |
| CH <sub>3</sub> + <i>i</i> -C <sub>4</sub> H <sub>9</sub>               | F.R.  | $3.5 \times 10^{16}$ | 83.6  | 85.0  | $3.8 \times 10^9$    | $1.5 \times 10^9$ |
|   | vib.  | $8.7 \times 10^{16}$ | 83.6  | 87.0  | $1.4 \times 10^9$    | $5.3 \times 10^8$ |
| CH <sub>3</sub> + <i>sec</i> -C <sub>4</sub> H <sub>9</sub>             | F.R.  | $7.9 \times 10^{16}$ | 81.4  | 82.1  | $4.3 \times 10^9$    | $1.1 \times 10^9$ |
|   | vib.  | $2.4 \times 10^{17}$ | 81.4  | 84.9  | $1.1 \times 10^9$    | $2.7 \times 10^8$ |
| C <sub>2</sub> H <sub>5</sub> + <i>i</i> -C <sub>3</sub> H <sub>7</sub> | F.R.  | $6.5 \times 10^{16}$ | 79.3  | 78.7  | $6.3 \times 10^9$    | $2.7 \times 10^9$ |
|   | vib.  | $2.4 \times 10^{17}$ | 79.3  | 82.0  | $1.1 \times 10^9$    | $4.7 \times 10^8$ |
| CH <sub>3</sub> + <i>neo</i> -C <sub>5</sub> H <sub>11</sub>            | F.R.  | $2.6 \times 10^{16}$ | 83.6  | 85.0  | $2.5 \times 10^9$    | $1.7 \times 10^9$ |
|   | vib.  | $6.3 \times 10^{16}$ | 83.6  | 86.5  | $1.1 \times 10^9$    | $7.5 \times 10^8$ |
| CH <sub>3</sub> + <i>t</i> -C <sub>5</sub> H <sub>11</sub>              | F.R.  | $1.4 \times 10^{17}$ | 78.4  | 78.5  | $1.1 \times 10^{10}$ | $3.7 \times 10^9$ |
|   | vib.  | $6.7 \times 10^{17}$ | 78.4  | 81.8  | $2.5 \times 10^9$    | $8.5 \times 10^8$ |
| C <sub>2</sub> H <sub>5</sub> + <i>t</i> -C <sub>4</sub> H <sub>9</sub> | F.R.  | $6.9 \times 10^{16}$ | 76.1  | 74.8  | $7.6 \times 10^9$    | $2.3 \times 10^9$ |
|   | vib.  | $4.4 \times 10^{17}$ | 76.1  | 78.8  | $1.3 \times 10^9$    | $4.1 \times 10^8$ |
| C <sub>2</sub> H <sub>5</sub> + <i>n</i> -C <sub>3</sub> H <sub>7</sub> | F.R.  | $5.3 \times 10^{16}$ | 81.5  | 81.9  | $2.2 \times 10^9$    | $7.1 \times 10^8$ |
|   | vib.  | $1.7 \times 10^{17}$ | 81.5  | 84.7  | $5.8 \times 10^8$    | $1.7 \times 10^8$ |
| CH <sub>3</sub> + <i>n</i> -C <sub>4</sub> H <sub>9</sub>               | F.R.  | $1.2 \times 10^{16}$ | 83.7  | 85.4  | $7.8 \times 10^8$    | $3.1 \times 10^8$ |
|   | vib.  | $2.7 \times 10^{16}$ | 83.7  | 87.3  | $2.8 \times 10^8$    | $1.1 \times 10^8$ |

<sup>a</sup> The recombination rates are given in units of liters mole<sup>-1</sup> sec<sup>-1</sup>, the  $A$ -factors are given in units of sec<sup>-1</sup>, and the activation energies are given in kcal/mole.

<sup>b</sup> The  $A$ -factors and activation energies were calculated at 1000°K except those for the isobutane and *n*-butane decomposition paths which were calculated at 800°K.

<sup>c</sup> The vibrator and free-rotor complex models were derived by treating all internal rotations in the molecules as free rotors in the  $k_{<E^*}>$  calculations, except for *n*-pentane where one ethyl internal rotation was treated as a 95 cm<sup>-1</sup> vibrator.

<sup>d</sup> These recombination rates were calculated at 400°K using tight radicals.

<sup>e</sup> These recombination rates were calculated at 400°K using loose radicals.

The  $A$ -factors for the free-rotor models range from  $10^{16.1}$  to  $10^{17.1}$  sec<sup>-1</sup>, and the  $A$ -factors for the vibrator models range from  $10^{16.4}$  to  $10^{17.8}$  sec<sup>-1</sup>. The free-rotor complexes and tight radicals give the best agreement with the estimated and measured experimental recombination rates, i.e.,  $\sim 10^{10}$  liters mole<sup>-1</sup> sec<sup>-1</sup> for all the recombinations except ethyl recombination, where the measured value is  $2.5 \times 10^{10}$  liters mole<sup>-1</sup> sec<sup>-1</sup> [53]. Nevertheless, most of the recombination rates calculated using these favorable extremes are significantly less than experimental and estimated recombination rates. If the tight radical structures are shown to be physically unrealistic, the correlation between the calculated and estimated experimental recombination rates would be worse by a factor of 2.5. Wage and Rabinovitch found a similar discrepancy between the decomposition and recombination rates for the ethane-methyl radical system [56]. Tsang has suggested that the discrepancy between the decomposition and recombination rates

could be removed by a negative activation energy of 2–3 kcal/mole for the recombination process [46]. Measurements of recombination rates over a large temperature range should help elucidate this matter.

The recombination rates and  $A$ -factors would be 1.8 and 2.2 times larger, respectively, if  $E_0$  values were raised by the 2 kcal/mole uncertainty in the measured bond dissociation energies. This would improve the correlation between the calculated and estimated recombination rates, but the correlation would still be less than satisfactory for the recombination reactions giving  $n$ -butane and  $n$ -pentane. In conclusion, the results of this study indicate that free-rotor complexes and tight radicals are required to bring the decomposition and estimated recombination rates into approximate agreement. More definite conclusions can be drawn once more reliable measurements of recombination rates and structures for larger radicals become available.

The free-rotor activated complex models predict that at this level of chemical activation, 120–125 kcal/mole, a change in the excitation energy  $\Delta E^*$  of  $3.8 \pm 0.1$  kcal/mole produces a twofold variation in  $k_{<E^*>}$  for the alkane decompositions studied here. Values of  $\Delta E^*$  predicted by the ratios of decomposition rate constants for the photolyses at 3660 and 4358 Å are presented in Table XII. These values were derived using the free-rotor complex models. Small variations from these values,  $\pm 0.2$  kcal/mole, would result using the vibrator complex models. The average of all the values of  $\Delta E^*$  is 3.0 kcal/mole. This quantity represents the difference in the amount of excess energy the singlet methylene radicals carry into their insertion products between the 3660 Å and 4358 Å photolyses. If the values of 5.8, 1.4, and 0.9 kcal/mole are not included, the average is 3.2 kcal/mole. A value of  $\Delta E^* = 3.0$  kcal/mole is satisfactory agreement with 3.5 kcal/mole measured by Simons and Taylor [7,8] for diazomethane-*cis*-butene-2 photolyses at 3660 and 4358 Å.

TABLE XII. Difference in  $E^*$  for photolyses at 3660 and 4358 Å.

| Molecule                | Substrate        | $\frac{k(3660 \text{ Å})}{k(4358 \text{ Å})}$ <sup>a</sup> |  | $\Delta E^*$ , kcal/mole <sup>b</sup> |
|-------------------------|------------------|--|--|---------------------------------------|
|                         |                  |  |  |                                       |
| Isobutane <sup>d</sup>  | propane          | 1.96   |  | 3.8                                   |
| <i>n</i> -Butane        | propane          | 3.19   |  | 5.8                                   |
| Neopentane <sup>d</sup> | isobutane        | 1.54   |  | 2.4                                   |
| Isopentane              | isobutane        | 1.85   |  | 3.2                                   |
| Isopentane              | <i>n</i> -butane | 1.29   |  | 1.4                                   |
| <i>n</i> -Pentane       | <i>n</i> -butane | 1.20   |  | 0.9                                   |
| Neohexane               | neopentane       | 1.89   |  | 3.4                                   |
|                         |                  |  |  | Average 3.0 (3.20) <sup>c</sup>       |

<sup>a</sup> This is the ratio of decomposition rate constants at 3660 Å to 4358 Å photolyses.

<sup>b</sup> The  $\Delta E^*$  values were calculated using the free rotor complex models at the median  $E_0$ . All reaction paths were considered in the evaluation of  $\Delta E^*$  for the molecules with more than one decomposition path.

<sup>c</sup> The average value with 5.8, 1.4, and 0.9 not included.

<sup>d</sup> These values derived from the results presented in refs. [5] and [6].

## Appendix I

### Molecular Collision Diameters

The effective molecular collision diameters  $s$  were calculated by multiplying the Lennard-Jones collision diameters [57] by the square root of the collision integral  $\Omega^{(2,2)*}(kT/\epsilon)$ . A uniform value of  $\epsilon/k = 325^\circ\text{K}$  was assumed for all the molecules as suggested by Rabinovitch et al. [13,14]. The Lennard-Jones collision diameters were taken from references [13], [14], [57], and [58]:

| Molecule  | $S, \text{\AA}$ |
|---|-----------------|
| $\text{O}_2$                                    | 4.55            |
| $\text{CH}_2\text{N}_2$                         | 6.55            |
| $\text{C}_3\text{H}_8$                          | 5.78            |
| <i>n</i> - $\text{C}_4\text{H}_{10}$            | 6.55            |
| <i>iso</i> - $\text{C}_4\text{H}_{10}$          | 6.50            |
| <i>n</i> - $\text{C}_5\text{H}_{12}$            | 7.32            |
| <i>iso</i> - $\text{C}_5\text{H}_{12}$          | 7.44            |
| <i>neo</i> - $\text{C}_5\text{H}_{12}$          | 7.92            |
| <i>neo</i> - $\text{C}_6\text{H}_{14}$          | 8.64            |
| $(\text{CH}_3)_3\text{SiH}$                     | 7.22            |
| $(\text{CH}_3)_4\text{Si}$                      | 8.64            |
| $\text{C}_2\text{H}_5(\text{CH}_3)_2\text{SiH}$ | 8.18            |

## Appendix II

### Radical Structures and Recombination Rate Calculations

A complete description of the radical models used in these calculations is given below. For the tight radical structures, the barriers to internal rotation, about bonds adjacent to the unpaired electron, were raised  $\sim 0.5$  kcal/mole above the value of the barrier in the related alkane. The entropies and partition functions given below are for the ideal gas standard state at 1 atm and  $400^\circ\text{K}$ . The ART expression for the rate of recombination of  $\text{R}_1 + \text{R}_2$  radicals is

$$k_r = \frac{kT}{h} \frac{Q^+/N}{[Q(\text{R}_1)/N][Q(\text{R}_2)/N]}$$

where  $E_0$  for recombination was taken to be zero and  $Q/N$  is the appropriate molecular partition function. The radical and complex partition functions were calculated using the following expression:

$$\ln(Q_T/N) = \frac{S_T^0}{R} - 4 - \frac{(H_T - H_0)_{\text{vib.}}}{RT} - \frac{(H_T - H_0)_{\text{i.r.}}}{RT}$$

where  $S_T^0$  is the total entropy at the temperature  $T$ , and  $[(H_T - H_0)_{\text{vib.}}]/RT$  and  $[(H_T - H_0)_{\text{i.r.}}]/RT$  are the vibrational and hindered internal rotational enthalpy functions, respectively. The entropies and the enthalpy functions of the hindered

rotors were taken from the tables of Pitzer [59,60]. Vibrational entropies and enthalpy functions were taken from tables of harmonic oscillator thermodynamic functions [61]. The internal rotational barriers for the radicals were derived from the internal rotational barriers of the related alkanes [36-38,47,48,62].

| Radical Models <sup>a</sup> |  |                       |           |
|-----------------------------|--|-----------------------|-----------|
| <i>Methyl Radical</i>       |  |                       |           |
| 3100(2)                     | $S^0_{400} = 49.4 \text{ e.u.}$                          |                       |           |
| 2930                        |  |                       |           |
| 1230(2)                     | $\ln(Q/N) = 20.41$                                       |                       |           |
| 611                         |  |                       |           |
| <i>Ethyl Radical</i>        |  |                       |           |
| 2960(5)                     |  |                       |           |
| 1440(4)                     |  |                       |           |
| 1155(2)                     | $I_r(\text{CH}_3) = 1.89 \times 10^{-40} \text{ g-cm}^2$ |                       |           |
| 820(2)                      |  |                       |           |
| 993                         |  |                       |           |
|                             | Tight  | Loose                 |           |
| CH <sub>3</sub> Torsion     | H.R. <sup>b</sup> ( $V_0 = 4.0$ ) <sup>c</sup>           | F.R. <sup>d</sup>     |           |
| $S^0_{400}$                 | 61.5 e.u.  | 62.3 e.u.             |           |
| $\ln(Q/N)$                  | 25.98  | 26.17                 |           |
| <i>n-Propyl Radical</i>     |  |                       |           |
| 2925(7)                     |  |                       |           |
| 1408(7)                     |  |                       |           |
| 1041(4)                     | $I_r(\text{CH}_3) = 3.82 \times 10^{-40} \text{ g-cm}^2$ |                       |           |
| 958(2)                      | $I_r(\text{CH}_2) = 2.52 \times 10^{-40} \text{ g-cm}^2$ |                       |           |
| 750                         |  |                       |           |
| 380                         |  |                       |           |
|                             | Tight  | Loose                 |           |
| CH <sub>3</sub> Torsion     | H.R. ( $V_0 = 3.4$ )                                     | H.R. ( $V_0 = 3.4$ )  |           |
| CH <sub>2</sub> Torsion     | H.R. ( $V_0 = 4.0$ )                                     | F.R.                  |           |
| $S^0_{400}$                 | 72.7 e.u.  | 74.1 e.u.             |           |
| $\ln(Q/N)$                  | 29.72  | 30.62                 |           |
| <i>Isopropyl Radical</i>    |  |                       |           |
| 2930(7)                     |  |                       |           |
| 1430(6)                     |  |                       |           |
| 1310(2)                     | $I_r(\text{CH}_3) = 4.9 \times 10^{-40} \text{ g-cm}^2$  |                       |           |
| 1050(2)                     |  |                       |           |
| 980(4)                      |  |                       |           |
| 380                         |  |                       |           |
|                             | Tight  | Loose                 |           |
| 2 CH <sub>3</sub> Torsions  | 250 cm <sup>-1</sup> <sup>e</sup>                        | H.R. ( $V_0 = 1.98$ ) | F.R.      |
| $S^0_{400}$                 | 70.1 e.u.  | 72.0 e.u.             | 73.1 e.u. |
| $\ln(Q/N)$                  | 28.66  | 29.31                 | 30.40     |
| <i>n-Butyl Radical</i>      |  |                       |           |

|                                       |   |                      |
|---------------------------------------|---|----------------------|
| 2918(9)                               |   |                      |
| 1394(10)                              |   |                      |
| 1166(2)                               | $I_r(\text{CH}_2) = 2.9 \times 10^{-40} \text{ g-cm}^2$             |                      |
| 997(4)                                | $I_r(\text{CH}_3) = 5.1 \times 10^{-40} \text{ g-cm}^2$             |                      |
| 789(3)                                | $I_r(\text{C}_2\text{H}_5)^f = 18.8 \times 10^{-40} \text{ g-cm}^2$ |                      |
| 431                                   |   |                      |
| 271                                   |   |                      |
|                                       | Tight   | Loose                |
| CH <sub>3</sub> Torsion               | H.R. ( $V_0 = 3.4$ )  | H.R. ( $V_0 = 3.4$ ) |
| C <sub>2</sub> H <sub>5</sub> Torsion | H.R. ( $V_0 = 4.0$ )  | H.R. ( $V_0 = 4.0$ ) |
| CH <sub>2</sub> Torsion               | H.R. ( $V_0 = 4.0$ )  | F.R.                 |
| $S^0_{400}$                           | 84.6 e.u.   | 88.7 e.u.            |
| $\ln(Q/N)$                            | 33.69   | 34.61                |

*sec-Butyl Radical*

|                                       |   |                      |
|---------------------------------------|---|----------------------|
| 2918(9)                               |   |                      |
| 1394(10)                              |   |                      |
| 1166(2)                               | $I_r(\text{CH}_3) = 5.3 \times 10^{-40} \text{ g-cm}^2$             |                      |
| 997(4)                                | $I_r(\text{CH}_3) = 5.3 \times 10^{-40} \text{ g-cm}^2$             |                      |
| 789(3)                                | $I_r(\text{C}_2\text{H}_5)^f = 18.8 \times 10^{-40} \text{ g-cm}^2$ |                      |
| 431                                   |   |                      |
| 271                                   |   |                      |
|                                       | Tight   | Loose                |
| CH <sub>3</sub> Torsion               | H.R. ( $V_0 = 3.4$ )  | H.R. ( $V_0 = 3.4$ ) |
| CH <sub>3</sub> Torsion               | H.R. ( $V_0 = 4.0$ )  | F.R.                 |
| C <sub>2</sub> H <sub>5</sub> Torsion | H.R. ( $V_0 = 4.5$ )  | H.R. ( $V_0 = 2.0$ ) |
| $S^0_{400}$                           | 84.2 e.u.   | 86.5 e.u.            |
| $\ln(Q/N)$                            | 33.52   | 34.89                |

*Isobutyl Radical*

|                         |   |                      |
|-------------------------|---|----------------------|
| 2932(9)                 |   |                      |
| 1410(9)                 | $I_r(\text{CH}_3) = 5.3 \times 10^{-40} \text{ g-cm}^2$ |                      |
| 1177(3)                 | $I_r(\text{CH}_3) = 5.3 \times 10^{-40} \text{ g-cm}^2$ |                      |
| 940(5)                  | $I_r(\text{CH}_2) = 2.9 \times 10^{-40} \text{ g-cm}^2$ |                      |
| 791                     |   |                      |
| 393(3)                  |   |                      |
|                         | Tight   | Loose                |
| CH <sub>3</sub> Torsion | H.R. ( $V_0 = 4.0$ )                                    | H.R. ( $V_0 = 4.0$ ) |
| CH <sub>3</sub> Torsion | H.R. ( $V_0 = 4.0$ )                                    | H.R. ( $V_0 = 4.0$ ) |
| CH <sub>2</sub> Torsion | H.R. ( $V_0 = 4.5$ )                                    | F.R.                 |
| $S^0_{400}$             | 81.4 e.u.   | 83.0 e.u.            |
| $\ln(Q/N)$              | 32.27   | 33.24                |

*t-Butyl Radical*<sup>a</sup>

|         |   |  |
|---------|---|--|
| 2960(9) |   |  |
| 1440(9) |   |  |
| 1300(2) |   |  |
| 990(6)  | $I_r(\text{CH}_3) = 5.1 \times 10^{-40} \text{ g-cm}^2$ |  |
| 710     |   |  |
| 480(2)  |   |  |
| 250     |   |  |

|                                       |  |                       |           |
|---------------------------------------|--|-----------------------|-----------|
|                                       | Tight  | Loose                 |           |
| 3 CH <sub>3</sub> Torsions            | 250 cm <sup>-1</sup> <sup>e</sup>                                      | H.R. ( $V_0 = 1.98$ ) | F.R.      |
| $S_{400}^0$                           | 77.2 e.u.  | 80.2 e.u.             | 81.9 e.u. |
| ln (Q/N)                              | 30.43  | 31.43                 | 33.16     |
| <i>Neopentyl Radical</i>              |  |                       |           |
| 2935(11)                              | $I_r(\text{CH}_3) = 5.3 \times 10^{-40}$ g-cm <sup>2</sup>             |                       |           |
| 1435(10)                              | $I_r(\text{CH}_3) = 5.3 \times 10^{-40}$ g-cm <sup>2</sup>             |                       |           |
| 1266(3)                               | $I_r(\text{CH}_3) = 5.3 \times 10^{-40}$ g-cm <sup>2</sup>             |                       |           |
| 964(8)                                | $I_r(\text{CH}_2) = 2.9 \times 10^{-40}$ g-cm <sup>2</sup>             |                       |           |
| 724                                   |  |                       |           |
| 384(5)                                |  |                       |           |
|                                       | Tight  | Loose                 |           |
| 3 CH <sub>3</sub> Torsions            | H.R. ( $V_0 = 4.3$ )   | H.R. ( $V_0 = 4.3$ )  |           |
| CH <sub>2</sub> Torsions              | H.R. ( $V_0 = 5.0$ )   | F.R.                  |           |
| $S_{400}^0$                           | 87.5 e.u.  | 88.7 e.u.             |           |
| ln (Q/N)                              | 33.85  | 34.21                 |           |
| <i>t-Pentyl Radical</i>               |  |                       |           |
| 2925(11)                              | $I_r(\text{CH}_3) = 5.3 \times 10^{-40}$ g-cm <sup>2</sup>             |                       |           |
| 1400(12)                              | $I_r(\text{CH}_3) = 5.3 \times 10^{-40}$ g-cm <sup>2</sup>             |                       |           |
| 1033(9)                               | $I_r(\text{CH}_3) = 5.3 \times 10^{-40}$ g-cm <sup>2</sup>             |                       |           |
| 781(2)                                | $I_r(\text{C}_2\text{H}_5)^f = 26.5 \times 10^{-40}$ g-cm <sup>2</sup> |                       |           |
| 413(3)                                |  |                       |           |
| 260                                   |  |                       |           |
|                                       | Tight  | Loose                 |           |
| CH <sub>3</sub> Torsion               | H.R. ( $V_0 = 3.4$ )   | H.R. ( $V_0 = 3.4$ )  |           |
| CH <sub>3</sub> Torsion               | H.R. ( $V_0 = 4.5$ )   | H.R. ( $V_0 = 1.98$ ) |           |
| CH <sub>3</sub> Torsion               | H.R. ( $V_0 = 4.5$ )   | H.R. ( $V_0 = 1.98$ ) |           |
| C <sub>2</sub> H <sub>5</sub> Torsion | H.R. ( $V_0 = 5.0$ )   | H.R. ( $V_0 = 2.5$ )  |           |
| $S_{400}^0$                           | 90.4 e.u.  | 93.2 e.u.             |           |
| ln (Q/N)                              | 35.0   | 36.1                  |           |

<sup>a</sup> All frequencies are in cm<sup>-1</sup>.

<sup>b</sup> H.R. = hindered rotor.

<sup>c</sup>  $V_0$  is the barrier to internal rotation given in kcal/mole.

<sup>d</sup> F.R. = free rotor.

<sup>e</sup> This frequency corresponds to an internal rotational barrier of 5 kcal/mole.

<sup>f</sup> This reduced moment of inertia was calculated using the method suggested by Herschbach et al. for unsymmetrical tops [51].

<sup>g</sup> The frequencies for the *t*-butyl radical are the same as those given by Halstead et al. [63].

### Bibliography

- [1] J. A. Bell and G. B. Kistiakowsky, *J. Amer. Chem. Soc.*, **84**, 3417 (1962).
- [2] M. L. Halberstadt and J. R. McNesby, *J. Amer. Chem. Soc.*, **89**, 3417 (1967).
- [3] G. Z. Whitten and B. S. Rabinovitch, *J. Phys. Chem.*, **69**, 4348 (1965).
- [4] B. S. Rabinovitch and D. W. Setser, *Advan. Photochem.*, **3**, 1 (1964).
- [5] R. L. Johnson, W. L. Hase, and J. W. Simons, *J. Chem. Phys.*, **52**, 3911 (1970).
- [6] W. L. Hase and J. W. Simons, *J. Chem. Phys.*, **54**, 1277 (1971).
- [7] J. W. Simons and G. W. Taylor, *J. Phys. Chem.*, **73**, 1274 (1969).

- [8] G. W. Taylor and J. W. Simons, *J. Phys. Chem.*, **74**, 464 (1970); G. W. Taylor and J. W. Simons, *Int. J. Chem. Kinet.*, **3**, 25 (1971).
- [9] W. L. Hase and J. W. Simons, *J. Chem. Phys.*, **52**, 4004 (1970).
- [10] J. H. Purnell and C. P. Quinn, *Can. J. Chem.*, **43**, 721 (1965).
- [11] J. Torok and S. Sandler, *Can. J. Chem.*, **47**, 3863 (1969); J. Torok and S. Sandler, *Can. J. Chem.*, **47**, 2707 (1969).
- [12] S. G. Lias and P. Ausloos, *J. Chem. Phys.*, **43**, 2748 (1965).
- [13] Y. N. Lin, Siu C. Chan, and B. S. Rabinovitch, *J. Phys. Chem.*, **72**, 1932 (1968); S. C. Chan, J. T. Bryant, L. D. Spicer, and B. S. Rabinovitch, *J. Phys. Chem.*, **74**, 2058 (1970).
- [14] S. C. Chan, B. S. Rabinovitch, J. T. Bryant, L. D. Spicer, T. Fujimoto, Y. N. Lin, and S. P. Pavlou, *J. Phys. Chem.*, **74**, 3160 (1970).
- [15] G. H. Kohlmaier and B. S. Rabinovitch, *J. Chem. Phys.*, **38**, 1709 (1963).
- [16] B. S. Rabinovitch and M. C. Flowers, *Quart. Rev.*, **18**, 122 (1964).
- [17] R. A. Marcus and O. K. Rice, *J. Phys. Colloid Chem.*, **55**, 894 (1951).
- [18] R. A. Marcus, *J. Chem. Phys.*, **20**, 359 (1952).
- [19] R. A. Marcus, *J. Chem. Phys.*, **43**, 2658 (1965).
- [20] D. W. Setser and B. S. Rabinovitch, *Can. J. Chem.*, **40**, 1425 (1962).
- [21] J. W. Simons and B. S. Rabinovitch, *J. Phys. Chem.*, **68**, 1322 (1964); D. W. Setser, B. S. Rabinovitch, and J. W. Simons, *J. Chem. Phys.*, **40**, 1751 (1964).
- [22] G. Z. Whitten and B. S. Rabinovitch, *J. Chem. Phys.*, **38**, 2466 (1963); G. Z. Whitten and B. S. Rabinovitch, *J. Chem. Phys.*, **41**, 1883 (1964); D. C. Tardy, B. S. Rabinovitch, and G. Z. Whitten, *J. Chem. Phys.*, **48**, 1427 (1968).
- [23] S. Glasstone, K. J. Laidler, and H. Eyring, "The Theory of Rate Processes," McGraw-Hill, New York, 1941.
- [24] American Petroleum Institute Research Project No. 44, Carnegie Institute of Technology, Pittsburgh, Pennsylvania, 1944-1952.
- [25] J. A. Kerr, *Chem. Rev.*, **66**, 465 (1966).
- [26] D. M. Golden and S. W. Benson, *Chem. Rev.*, **69**, 125 (1969).
- [27] S. W. Benson, "Thermochemical Kinetics. Methods for the Estimation of Thermochemical Data and Rate Parameters," Wiley, New York, 1968.
- [28] R. C. Weast and S. M. Selby, "Handbook of Chemistry and Physics," The Chemical Rubber Co., Cleveland, Ohio, 1969.
- [29] M. C. Lin and K. J. Laidler, *Trans. Faraday Soc.*, **64**, 79 (1968).
- [30] C. Steel and K. J. Laidler, *J. Chem. Phys.*, **34**, 1827 (1961).
- [31] H. M. Frey and R. Walsh, *Chem. Rev.*, **69**, 103 (1969).
- [32] S. W. Benson, *Advan. Photochem.*, **2**, 1 (1964).
- [33] J. H. Schachtschneider and R. G. Snyder, *Spectrochim. Acta*, **19**, 117 (1963).
- [34] R. G. Snyder and J. H. Schachtschneider, *Spectrochim. Acta*, **21**, 1969 (1965).
- [35] D. E. Milligan and M. E. Jacox, *J. Chem. Phys.*, **47**, 5146 (1967); R. W. Fessenden, *J. Phys. Chem.*, **71**, 74 (1967); J. M. Riveros, *J. Chem. Phys.*, **51**, 1269 (1970); G. Herzberg and J. Shoosmith, *Can. J. Phys.*, **34**, 523 (1956); G. Herzberg, *Proc. Roy. Soc., Ser. A*, **262**, 291 (1961).
- [36] S. Weiss and G. E. Leroi, *J. Chem. Phys.*, **48**, 962 (1968).
- [37] S. Weiss and G. E. Leroi, *Spectrochim. Acta*, **25A**, 1759 (1969).
- [38] J. R. Durig, S. M. Craven, and J. Bragin, *J. Chem. Phys.*, **52**, 2046 (1970); J. R. Durig, S. M. Craven, and J. Bragin, *J. Chem. Phys.*, **53**, 38 (1970).
- [39] R. W. Fessenden, *J. Chim. Phys.*, **61**, 1570 (1964); R. W. Fessenden, *J. Phys. Chem.*, **71**, 74 (1967); T. Gillbro, P. O. Kinell, and A. Lund, *J. Phys. Chem.*, **74**, 4167 (1969); H. Fischer, *J. Phys. Chem.*, **73**, 3834 (1969).
- [40] F. A. Rushworth, *Proc. Roy. Soc., Ser. A*, **222**, 526 (1954).

- [41] N. Norman and H. Mathieson, *Acta Chem. Scand.*, **18**, 353 (1964); Central Institute for Industrial Research, Final Technical Report, Publication No. 334, Blindern, Oslo, 1961; J. A. Brivati, K. D. J. Root, M. C. R. Symons, and D. J. A. Tinling, *J. Chem. Soc., A*, 1942 (1969).
- [42] D. B. Chesnut, *J. Chem. Phys.*, **29**, 43 (1958); R. Fantechi and G. A. Helcke, *J. Chem. Soc. A*, 1294 (1970); Z. Luz, *J. Chem. Phys.*, **48**, 4186 (1968).
- [43] J. H. Purnell and C. P. Quinn, *Proc. Roy. Soc., Ser. A*, **270**, 267 (1962).
- [44] N. H. Sagert and K. J. Laidler, *Can. J. Chem.*, **41**, 838 (1963).
- [45] A. F. Trotman-Dickenson, "Gas Kinetics," Butterworth, London, 1955, p. 125.
- [46] Wing Tsang, *Int. J. Chem. Kinet.*, **1**, 245 (1969).
- [47] J. P. Lowe, "Progress in Physical Organic Chemistry," Vol. 6, Interscience, New York, 1968, p. 1.
- [48] K. S. Pitzer, *Ind. Eng. Chem.*, **36**, 829 (1944).
- [49] K. S. Pitzer, *J. Chem. Phys.*, **5**, 473 (1937).
- [50] J. E. Piercy and M. G. Seshagiri Rao, *J. Chem. Phys.*, **46**, 3951 (1967).
- [51] D. R. Herschbach, H. S. Johnston, K. S. Pitzer, and R. E. Powell, *J. Chem. Phys.*, **25**, 736 (1956).
- [52] J. H. Purnell and C. P. Quinn, *J. Chem. Soc.*, 4049 (1964).
- [53] A. Shepp and K. O. Kutschke, *J. Chem. Phys.*, **37**, 700 (1962).
- [54] J. E. Kilpatrick and K. S. Pitzer, *J. Amer. Chem. Soc.*, **68**, 1066 (1946).
- [55] D. A. Leathard and J. H. Purnell, In "Annual Review of Physical Chemistry, Vol. 21," H. Eyring, Ed., Annual Reviews Inc., New York, 1970, p. 217.
- [56] E. V. Waage and B. S. Rabinovitch, *Int. J. Chem. Kinet.*, **3**, 105 (1971).
- [57] J. O. Hirschfelder, C. F. Curtiss, and R. B. Bird, "Molecular Theory of Gases and Liquids," Wiley, New York, 1954.
- [58] J. C. McCoubrey and N. M. Singh, *J. Phys. Chem.*, **67**, 517 (1963).
- [59] K. S. Pitzer and W. D. Quinn, *J. Chem. Phys.*, **10**, 428 (1942).
- [60] G. N. Lewis and M. Randall, revised by K. S. Pitzer and L. Brewer, "Thermodynamics," McGraw-Hill, New York, 1961, p. 441.
- [61] H. L. Johnston, L. Savedoff, and J. Belzer, "Contributions to the Thermodynamic Functions by a Planck-Einstein Oscillator in One Degree of Freedom," Office of Naval Research, Department of the Navy, Washington, D.C., 1949.
- [62] J. P. Lowe, *J. Chem. Phys.*, **51**, 832 (1969).
- [63] M. P. Halstead, R. S. Konar, D. A. Leathard, R. M. Marshall, and J. H. Purnell, *Proc. Roy. Soc., Ser. A*, **310**, 525 (1969).

Received May 5, 1971.